Conformational analysis by NMR spectroscopy, molecular dynamics simulation in water and X-ray crystallography of glutamic acid analogues: isomers of 1-aminocyclopentane-1,3-dicarboxylic acid

Valéry Larue,[a] Josyane Gharbi-Benarous,[a,b] Francine Acher,[a] Giovanni Valle,[c] Marco Crisma,[c] Claudio Toniolo,[c] Robert Azerad[a] and Jean-Pierre Girault*,[a]

[a] *Université René Descartes-Paris V, Laboratoire de Chimie et Biochimie Pharmacologiques et Toxicologiques (URA 400 CNRS), 45 rue des Saints-Pères, 75270 Paris Cedex 06, France*

[b] *Université Denis Diderot-Paris VII, UFR Chimie, 2 Place Jussieu, F-75251 Paris Cedex 05, France*

[c] *University of Padova, Biopolymer Research Center, C.N.R., Department of Organic Chemistry, 35131 Padova, Italy*

The conformational analysis of two isomeric glutamic acid analogues containing a cyclopentane ring, substituted in position 1 by an amino and a carboxyl group, and in position 3 by a second carboxyl group has been carried out in an aqueous environment, by ^1H and ^{13}C NMR spectroscopy, and molecular dynamics (MD). The X-ray structure of the *trans*-isomer is included in this study. These *cis* and *trans* analogues may display envelope **E** or 'twist' **T** conformations in aqueous solution. The definition of *cis* and *trans* is relative to the arrangement of the carboxyl function. This study shows four conformational families **I–IV** with characteristic distances between the potentially active functional groups, α-NH_3^+–γ-CO_2^- and α-CO_2^-–γ-CO_2^-. At physiological pH, the amino group in the *cis*-isomer **1** is found to be axial (^{2}**E** or $\mathbf{E}_3$ conformers), both carboxyl groups being in equatorial positions to reduce the steric energy (type **II**). In the *trans*-isomer **2**, a 1,3-electrostatic attraction stabilizes the $\mathbf{E}_1$ or ^{5}**E** conformers with the α-NH_3^+ and γ-CO_2^- in an axial or isoclinal position (type **I**). Conversely, at isoelectric pH when the 3-carboxylate group is protonated, each isomer is represented by new privileged conformations. The *cis*-isomer **1** exhibits a $\mathbf{E}_5$ conformation in which the 1-carboxylate group, α-CO_2^-, is axial and stabilized by an electrostatic interaction with the 3-carboxyl group, γ-CO_2H, less equatorial (type **IV**). For the *trans*-isomer **2**, the steric parameters favour the $\mathbf{E}_2$ or ^{3}**E** conformations, in which the two carboxy groups are shown to be equatorial or isoclinal and the amino group axial (type **III**).

The data obtained may be considered as important elements in the recognition features of these glutamic acid analogues in biological systems (NMDA or ACPD receptors of the central nervous system, glutamine synthetase, D-glutamate-adding enzyme, *etc.*).

Considerable recent interest has been generated in the pharmacology of acidic amino acids related to glutamic acid because of the perceived role of these compounds in various biological functions [*e.g.* (*i*)–(*iii*)]. (*i*) As synaptic transmitters in the mammalian central nervous system.[1] At the present time, the excitatory amino acid receptors are believed to be of different types, those which have a particular affinity for NMDA (*N*-methyl-D-aspartic acid) or AMPA [α-amino-3-hydroxy-5-methylisoxazole-4-propionic acid] or KA (kainic acid), respectively[2] and in addition to these ionotropic receptors, the metabotropic L-Glu receptors.[3] Recently, molecular cloning studies have revealed a family of metabotropic receptors termed mGluR1 to mGluR6.[4] (*ii*) Previously, as substrates of glutamine synthetase.[5] (*iii*) More recently, as substrates or inhibitors of the D-glutamate-adding enzyme from *Escherichia coli*.[6] This last enzyme belongs to the biosynthesis pathway of the bacterial cell wall peptidoglycan[7] and has been purified recently.[8]

One of the methods of choice, to analyse the diversity of the receptors that mediate the neuronal events, to elucidate the conformation which binds to the active site of the glutamine synthetase, or to investigate the structural requirements of the D-glutamate-adding enzyme towards its amino acid substrate, is to produce rigid analogues of glutamic acid. Ring closure imposes conformational constraints and limitations not existing in linear flexible systems [Fig. 1(*a*)]. The introduction of conformationally restricted analogues of natural amino acids in substrates or inhibitors has already proved helpful for studies of the geometry of binding sites.[5,9,10]

Two isomeric glutamic acid analogues containing a cyclohexane ring [the *cis*- and *trans*-C6, Fig. 1(*b*)], substituted at position 1 by an amino and a carboxyl group, and in position 3 by a second carboxyl group have already been tested for some biological properties in comparison to glutamic acid: the (±)-*cis*-derivative is about 10 times more potent than the (±)-*trans*-isomer as an agonist of non-NMDA ionotropic receptors of the central nervous system;[11] compound (L)-*cis* is a substrate of glutamine synthetase, while (L)-*trans* is not;[5] the (D,L)-*trans*-isomer was shown recently to be a competitive substrate for UDP-Mur-Nac-L-Ala-D-Glu synthetase.[6] The conformations of these two glutamic acid analogues (*cis*- and *trans*-1-aminocyclohexane-1,3-dicarboxylic acids), have been investigated by X-ray crystallography, ^1H and ^{13}C NMR spectroscopy in an aqueous environment, and molecular dynamics (MD).[12] These analogues exclusively exhibit chair conformations in aqueous solution. When the two carboxyl groups are *cis* they were shown to be equatorial and the amino group was shown to be axial, independently of charge and pH. However, in the *trans*-isomer the 1-amino and 3-carboxyl groups are equatorial except about neutral pH, where there is an equilibrium with another conformer, in which the 1-ammonium and the 3-carboxylate groups are

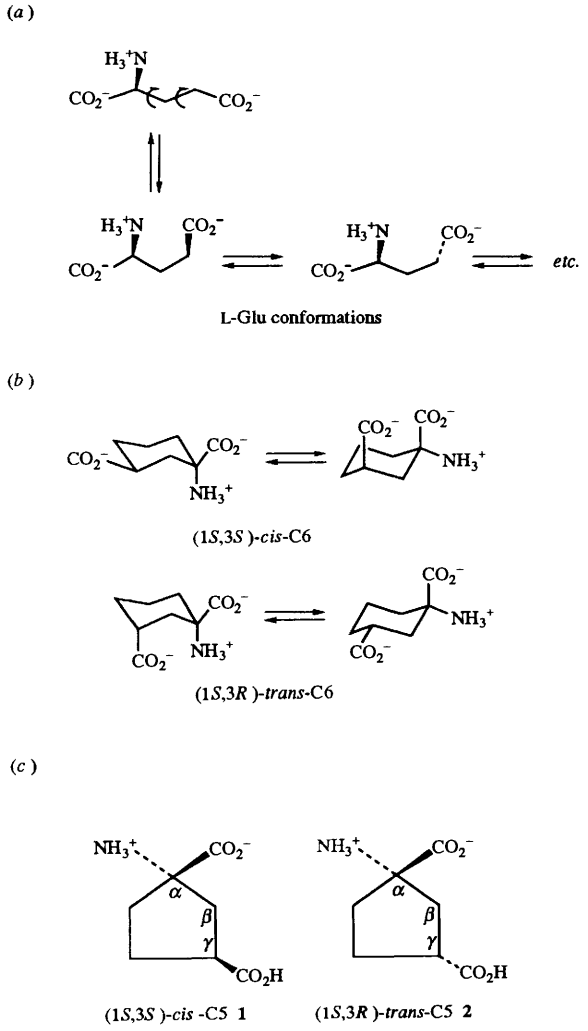

Fig. 1 (*a*) Extended and folded conformations of L-Glutamic acid around neutral pH; (*b*) predominant conformations of *cis*- and *trans*-cyclohexane derivatives in aqueous solution at pH 7; (*c*) structure of the amino acid analogues studied at pH 4, *cis*-C5 **1** and *trans*-C5 **2** [isomers α-(*S*) represented, zwitterions]

axial and stabilized by a large electrostatic interaction or hydrogen bond [Fig. 1(*b*)].

Another set of experiments is centred around cyclopentane analogues of the amino acid L-Glu. These molecules are more flexible than the *cis*- and *trans*-C6 and they could adopt a better geometry for the binding site. The *cis*- and *trans*-1-aminocyclopentane-1,3-dicarboxylic (ACPD) acids hereafter named *cis*-C5 **1** and *trans*-C5 **2**, respectively [Fig. 1(*c*)], have already been tested. The results indicate a high degree of specificity for the interaction of each isomer. Among the two isomers, only the (1*S*,3*S*)-*cis*-C5 **1** was a substrate of glutamine synthetase. For UDP-Mur-Nac-L-Ala-D-Glu synthetase, the (±)-*trans*-C5 **2** was shown recently to be the only active isomer.[6] The (1*R*,3*R*)-*cis*-(dicarboxylic)-ACPD isomer **1** is an agonist of NMDA receptor[13] while the (1*S*,3*R*)-*trans*-(dicarboxylic)-ACPD isomer **2** is a specific agonist of metabotropic glutamate receptors (ACPD receptor).[14] Both enantiomers (1*S*,3*R*)- and (1*R*,3*S*)-*trans*-ACPD **2** stimulated responses in rat cerebellum RNA-injected Xenopus oocytes, the second isomer being much weaker.[15] The selective agonist *trans*-ACPD has allowed the metabotropic excitatory amino acid receptors to be distinguished pharmacologically from ionotropic receptors (NMDA, AMPA, KA)[2] and only a few specific drugs were shown to interact with the metabotropic Glu receptors.

Selective binding of conformationally restricted analogues implies that glutamate may bind to each receptor in a distinct conformation.[1] Previous analyses indicate that the two carboxylic groups are essential and must be present within a prescribed proximity and that a group capable of bearing at least partial positive charge such as an amino group should also be present. NMDA agonist and competitive antagonist pharmacophore models were described[16] suggesting the possibility of different binding modes at the receptor by molecular modelling. Solvent and charges were not considered in these calculations. The resulting geometries were dependent on the conditions employed and may be compromised by such simplifications given that biological binding studies depend strongly upon experimental conditions.

The following study of *cis* **1**- and *trans* **2**-C5[13a,17] has been undertaken [Fig. 1(*c*)] by NMR spectroscopy and molecular dynamics. As MD calculations deal with the energy and geometry of individual conformations, whereas NMR data are averaged over different conformations, this study serves to correlate the two methods.

The computational investigation was undertaken in water in order to elucidate the conformational characteristics in a biological-type environment and then provide information on the dynamic behaviour of the different isomers as well as their hydration.

A conformational search at physiological pH, on the molecules whose ionized functional groups are γ-CO_2^-, α-CO_2^- and α-NH_3^+ was performed by NMR spectroscopy and MD. However, we considered that the arrangement of these ionized basic and acidic residues in the amino acid analogues bound to the receptor protein might not correspond precisely to the arrangement of these opposite charges on the free agonists. The receptor itself may present numerous contact points, some of them carrying partial electric charges, others being acceptors or donors of protons. A complex network of interactions (electrostatic, hydrogen bonds) involving, in addition, water molecules represents a schematic model for the receptor.[16b] Thus, our study includes an extensive conformational analysis in water at different pH values (*i*) the case of the γ-carboxylate group bearing a proton (isoelectric pH = 3, zwitterionic form) that can provide a γ-carboxylic group (γ-CO_2H) which possesses a potential proton donor hydroxy group and (*ii*) the case of an amino group carrying no formal charge (pH = 11), and hence it was interesting to examine the conformational change induced by the electrostatic field generated by different polarity of these molecules.

The results of this study should lead to a detailed understanding of their conformation in solution. But the conformational problems posed by the saturated five-membered ring are far more complex than those of the six-membered ring. The combination of NMR analysis with molecular dynamics and mechanics calculations could lead us to a complete assignment of each conformer and the conformation of the molecules in solution.

Results and discussion

In cyclopentane, the strain in the molecule is partly relieved by puckered conformations. Two flexible forms of cyclopentane exist, namely the so-called, envelope **E** and half-chair or twist **T** forms.[18a] These forms are represented in Fig. 2(*a*). In these conformers, the following types of exocyclic bonds have been recognized: equatorial (e), axial (a) and the so-called isoclinal (i) bonds.[18b] The two conformers **E** and **T** are extremes of symmetry in what is known as the pseudorotational circuit of cyclopentane. If in a structure ^{1}**E** the out-of-plane carbon (arbitrarily designated C-1 here) is pushed down, another envelope $\mathbf{E}_1$ is reached [Fig. 2(*b*)]. If the motion is continued C-1 is pushed down together with C-2 and a half-chair $^1\mathbf{T}_2$ is

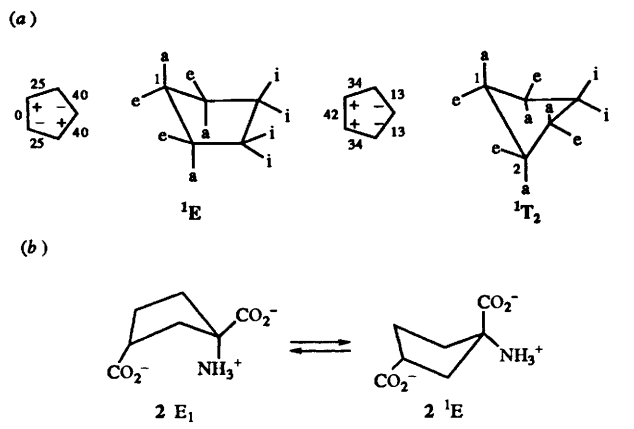

Fig. 2 (*a*) Considered conformations for cyclopentane. The forms, envelope **E** and half-chair or twist **T** are represented in perspective drawing, as well as in the conventional formula indicating the approximate values of the torsion angles and their sign and with the following types of exocyclic bonds: equatorial (e), axial (a), and the so-called isoclinal (i) bonds. The former has four carbons in the same plane, in contrast, the half-chair has three coplanar carbon atoms, one above and one below ($^1\mathbf{T}_2$); (*b*) Conformations envelope **E** for *trans*-C5 **2** at pH 7. Conformational equilibrium between the structure $^1\mathbf{E}$ and another envelope $\mathbf{E}_1$ when the out-of-plane C-1 is pushed down.

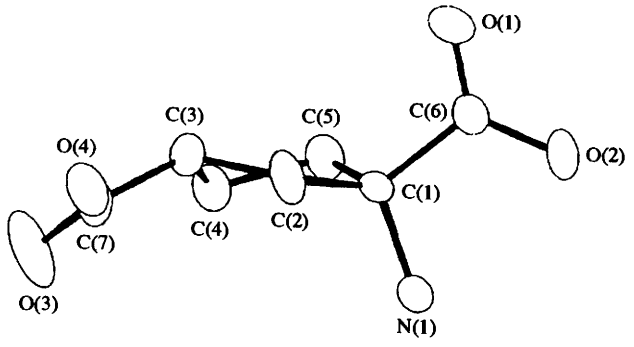

Fig. 3 ORTEP drawing of the (*S,R*)-enantiomer of *trans*-C5 **2**

obtained [Fig. 2(*a*)].[18c] The envelope and the half-chair forms interconvert by the pseudorotation process which is almost of constant strain, and thus many of these conformations have approximately the same energy.[19a] An accurate description of the ring will be given by the use of the two pseudorotation parameters,[19b] the phase, *P*, and the puckering, τ_m.

However, as three acidity functions are present in these compounds (pK_a = 2.2, 4.3, 9.7), the charges of the groups and their protonation depend on the pH of the solution: four predominant forms must be taken into account for the study in aqueous solution from **1** (pH ≤ 4) to **3** (pH ≥ 9). The preferred conformation may depend on these charges because of the electrostatic interactions or hydrogen bonding implied. Thus, it is necessary to analyse the conformations at different pH values. The first number indicates the isomer [*cis* **1**, *trans* **2**, see Fig. 1(*c*)], in the second one the predominant form in the pH zone considered (from acidic zone **1** to alkaline zone **3**), and the letter represents the chair or half-chair conformation (**E** or **T**, Fig. 2). All products are racemic but in the discussion and schemes, the C-1 carbon will be always of (*S*)-configuration. So, the **a** face of the cyclopentane ring is that which contains the carboxyl group in position 1.

X-Ray crystallography

trans-C5 **2** Monohydrate (Fig. 3), crystallized at pH 4.5 and is zwitterionic, with the α-amino group protonated. Bond distances at the α- and γ-carboxy groups are of comparable length [C(6)–O(1) 1.224(9), C(6)–O(2) 1.287(8) Å, *cf.* C(7)–O(3) 1.219(9) and C(7)–O(4) 1.313(9) Å]. These values alone do not allow us to place unambiguously the negative charge on either group. However, we tentatively assign the carboxylate group to the α-substituent on the basis of the location on a difference-Fourier map of a hydrogen atom linked to O(4).

Table 1 Torsion angles (°) for the (*S,R*)-enantiomer of *trans*-C5 **2**

O(2)–C(6)–C(1)–N(1)	14.3	C(1)–C(5)–C(4)–C(3)	40.2
O(1)–C(6)–C(1)–N(1)	−165.1	C(5)–C(4)–C(3)–C(2)	−36.3
O(1)–C(6)–C(1)–C(5)	74.5	C(4)–C(3)–C(2)–C(1)	18.7
O(1)–C(6)–C(1)–C(2)	−42.8	C(5)–C(1)–C(2)–C(3)	6.2
O(2)–C(6)–C(1)–C(5)	−106.1	C(3)–C(2)–C(1)–N(1)	−112.0
O(2)–C(6)–C(1)–C(2)	136.6	C(4)–C(5)–C(1)–N(1)	89.7
O(3)–C(7)–C(3)–C(2)	−135.3	C(7)–C(3)–C(2)–C(1)	145.9
O(3)–C(7)–C(3)–C(4)	−14.2	C(7)–C(3)–C(4)–C(5)	160.7
O(4)–C(7)–C(3)–C(2)	45.9	C(6)–C(1)–C(2)–C(3)	126.4
O(4)–C(7)–C(3)–C(4)	166.9	C(6)–C(1)–C(5)–C(4)	−150.9

In the crystals both enantiomers (*S,R* and *R,S*) are present. In Table 1 torsion angles are given pertaining to the (*S,R*) enantiomer shown in Fig. 3. The conformation of the cyclopentyl ring can be described as intermediate between the envelope $\mathbf{E}_4$ and twist $^5\mathbf{T}_4$ conformations, with a puckering amplitude q_2 = 0.393(8) Å.[19a] From the torsion angles giving the disposition of the substituents relative to the ring, reported in Table 1, it can be deduced that the α-ammonium group occupies the axial position, while both α-carboxylate and γ-carboxy groups are equatorial.

Packing of the molecules is achieved through a network of hydrogen bonds. The O(4)–H group is strongly hydrogen-bonded to the O(2) atom of a (1/2 + *x*, 3/2 − *y*, 1 + *z*) symmetry related molecule, being the O(4)···O(2) distance 2.560(7) Å. The α-ammonium group acts as hydrogen bond donor to a (*x*, *y*, 1 + *z*) symmetry related O(1) atom and to the oxygen atom of a (1/2 − *x*, *y* − 1/2, 1 − *z*) symmetry related co-crystallized water molecule. The N(1)···O(1) and N(1)···O(W) distances are 2.773(8) and 2.783(11) Å, respectively. Finally, the water molecule is also hydrogen-bonded to the O(3) atom of a (*x*, *y*, −1 + *z*) symmetry related amino acid molecule, with an O(W)···O(3) separation of 2.868(11) Å.

NMR spectroscopy

The study was carried out on samples dissolved in deuterium oxide at room temperature (see Experimental). Several pH values are considered, except for the carbon resonances which are examined only at pH 7 due to solubility constraints and to the particular interest of this pH.

The assignments have been made using 1D ^{1}H and ^{13}C (^{1}H decoupled and DEPT-135)[20] spectra, and 2D homonuclear (COSY-60)[21] and heteronuclear (F_1 decoupled)[22] shift correlations. The results are presented in Table 2. The conformational analysis is based on the vicinal $^3J_{H,H}$ coupling constants. Interpretation of these couplings permits qualitative and quantitative conclusions to be made about the shapes of these rings. We report in this paper the complete analysis of the proton spectra. 3-H has a higher resonance frequency than the other protons. Thus, in order to make a complete analysis of the seven-spin system of molecules **1** and **2**, two separate systems, four-spin and two-spin (AB), were isolated by double irradiation at the 3-H resonance frequency. The spectra of compounds **1** and **2** are readily analysed under this condition and the vicinal coupling constants were obtained from these spectra by iterative techniques on a spectral simulation (PANIC). Fig. 4 presents the observed and calculated spectra for both isomers of cyclopentane derivatives at pH 7.0 (**1 2** and **2 2**). Determination of heteronuclear ^{13}C–^{1}H coupling constants by the selective 2D INEPT experiment[23] is especially helpful for 3-H bonds in order to determine the relative positions of the substituents on the C5-ring (Fig. 5).

Table 2 ^1H chemical shifts in D_2O at various pH values (δ/[$^2H_4$]TSP error 0.01 ppm) and ^{13}C chemical shifts in D_2O at pH 7 (δ_C/[$^2H_4$]TSP); H noted a or b according to the geometrical isomerism of the proton (Ha and NH_3^+ *trans*; Hb and NH_3^+ *cis*)

	cis-C5 **1**				*trans*-C5 **2**			
	11[a] pH 3	**13**[a] pH 11	**12**[a] pH 7	**12**[b] pH 7	**21**[a] pH 3	**23**[a] pH 11	**22**[a] pH 7	**22**[b] pH 7
1				69.4				69.6
2a	2.51	2.17	2.37	42.7	2.53	2.37	2.37	42.6
b	2.26	1.90	2.20		2.15	1.69	2.10	
3a				48.8	3.20	2.83	3.02	49.6
b	3.15	2.91	2.93					
4a	2.10	1.90	1.97	32.3	2.27	2.02	2.24	32.8
b	2.21	2.10	2.14		2.05	1.69	1.97	
5a	2.36	2.20	2.37	38.3	2.26	2.05	2.30	38.4
b	1.96	1.65	1.89		2.02	1.87	2.04	
6				180.0				180.1
7				187.3				187.3

[a] ^1H. [b] ^{13}C.

Table 3 $^1H,^1H$ and $^1H,^{13}C$ coupling constants in D_2O (Hz, error 0.5 Hz) values confirmed by simulation of the signals (program PANIC); 3-H noted a (for *trans*-C5 **2**) or b (for *cis*-C5 **1**) according to the geometrical isomerism of the proton (Ha and NH_3^+ *trans*; Hb and NH_3^+ *cis*)

		cis-C5 **1**		*trans*-C5 **2**			
		12 pH 7	**11** pH 3	X-ray[a]	**22** pH 7	**21** pH 3	**23** pH 11
J/Hz							
^2J	2a, 2b	−15.0	−14.0		−14.5	−14.0	−14.0
	4a, 4b	−14.0	−12.5		−12.0	−12.0	−12.5
	5a, 5b	−15.0	−14.0		−14.5	−14.0	−14.0
^3J	3, 2a	12.0	10.0	10.7	8.5	9.0	8.0
	3, 2b	6.5	9.0	8.3	4.5	7.0	10.0
	3, 4a	10.0	8.0	6.5	8.0	9.0	8.0
	3, 4b	8.5	9.0	12.8	5.0	7.0	10.0
	4a, 5a	12.0	8.0	6.5	7.5	7.5	8.0
	4a, 5b	7.0	7.0	0.7	4.0	4.0	8.0
	4b, 5a	3.5	5.0	12.7	8.5	9.0	7.0
	4b, 5b	8.0	8.0	5.5	7.0	8.0	10.0
^3J	3-H, C-1	<1	—	0.5	3.5	—	—
	3-H, C-5	<1	—	1.1	2.5	—	—

[a] The coupling constants values $^3J_{HH}$ calculated by Altona's equations[24] and the $^3J_{CH}$ values by a Karplus type-equation:[25] $^3J_{CH} = 5.7 \cos^2 \varphi - 0.6 \cos \varphi + 0.5$.

The coupling constants derived from these analyses are given in Table 3. The relative position **a** or **b** for the different protons is defined by the nuclear Overhauser enhancement (NOE) experiment results in 1D (NOE difference) involving 3-H (3a-H in *trans*-C5 **2** and 3b-H in *cis*-C5 **1**).

***cis*-C5 1.** We can deduce the axial or equatorial position of 3b-H from the spin system value of its neighbouring nuclei 4a- and 2a-H. The two large values of the coupling constants $J_{H(2a)H(3b)}$ and $J_{H(3b)H(4a)}$ in **1 2** at pH 7.0 (12.0 and 10.0 Hz) show that 2a-, 3b- and 4a-H are axial and thus, the 3-carboxy group is equatorial. In this molecule, the ammonium group may be axial and there is no 1,3-interaction between the two equatorial 1,3-carboxylate groups on C-1 and -3. This result was confirmed by spectral simulation (Fig. 4). These observations allow us to propose for **1** a conformational structure with 2a-, 3b- and 4a-H axial, the polar groups CO_2^- equatorial on C-1 and -3 and despite its bulkiness, the ammonium group axial on C-1. At the other pH values tested, the coupling constants are very similar to those of **1 2**. At pH 3.0 in the isomer **1 1**, where the 3-carboxy group and the 1-amino group are protonated, the coupling constant $J_{H(2a)H(3b)} = 10$ Hz shows that 2a- and 3b-H are *trans* and biaxial, but $J_{H(3b)H(4a)} = 8.0$ Hz is not a characteristic value. The decrease of these two large coupling constants reveals that 3b-H is partially axial, in agreement with an isoclinal proton or a conformational equilibrium. Thus, the previous ring conformation is similar to that observed for these molecules, but the isomer **1 1** may be found as a mixture of the two conformations—one with α-CO_2^- or γ-CO_2H groups diequatorial, α-NH_3^+ axial; and another one where the γ-CO_2H group is less equatorial on C-3, and stabilized by an electrostatic interaction with α-CO_2^- axial group (α-NH_3^+ equatorial on C-1). At alkaline pH, the conformation **1 3** could not be analysed owing to an observable broadening under the exchange process which affects the NMR spectrum.

We conclude that the *cis*-C5 **1** will adopt a predominant conformation with the minimal steric hindrance due to the two equatorial 1,3-carboxylate groups. Therefore, at pH 3.0 the coupling constants are averaged: the preferred conformer is still predominant, but in conformational equilibrium with a conformer in which 3b-H is isoclinal (γ-CO_2H pseudo-axial).

All these conclusions will be further tested using MD experiments. In Table 4, we have reported the torsion angles and the coupling constants calculated by Altona's equation[24] in the *cis*-C5 **1** isomers from the minimized structures generated by MD.

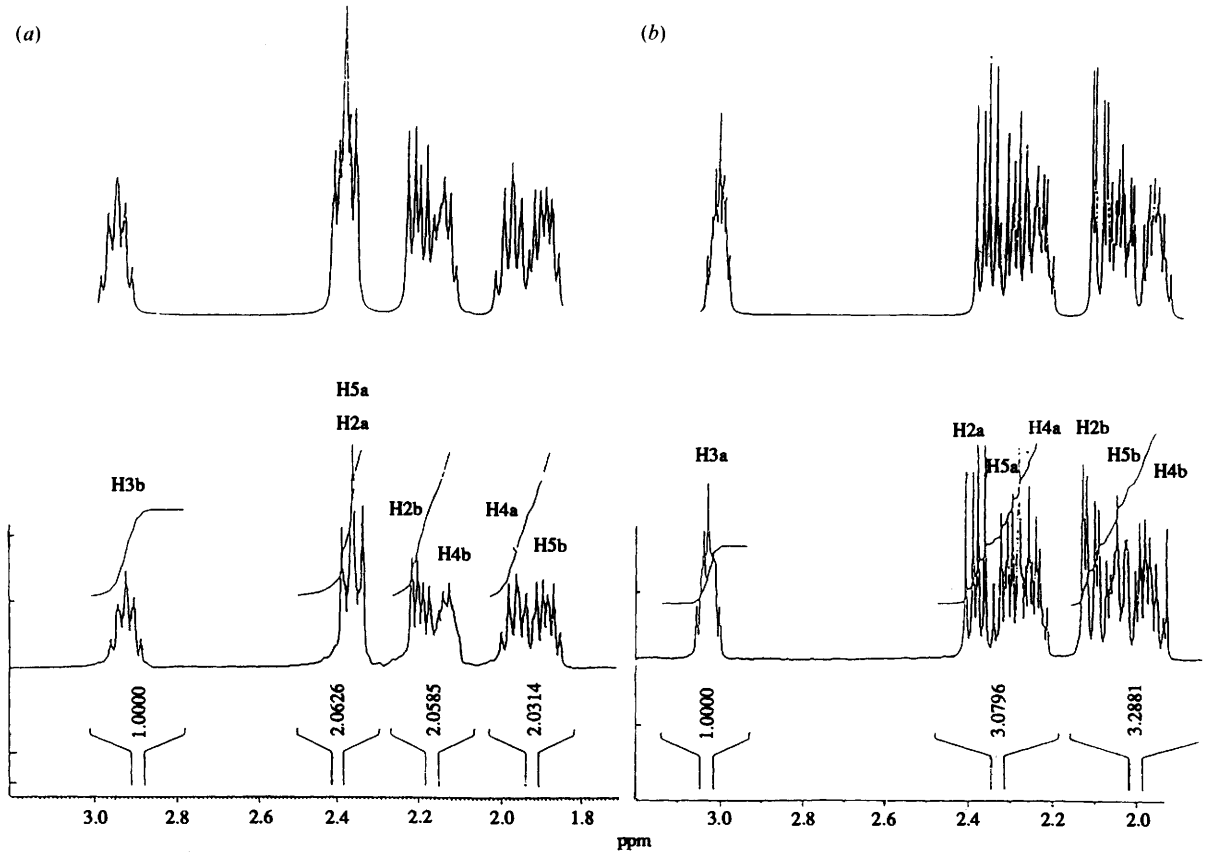

Fig. 4 Details of the 500 MHz ^{1}H spectrum (represented at pH 7) and simulation of the signals (top) for (*a*) *cis*-C5 **1** and (*b*) *trans*-C5 **2** in aqueous solution

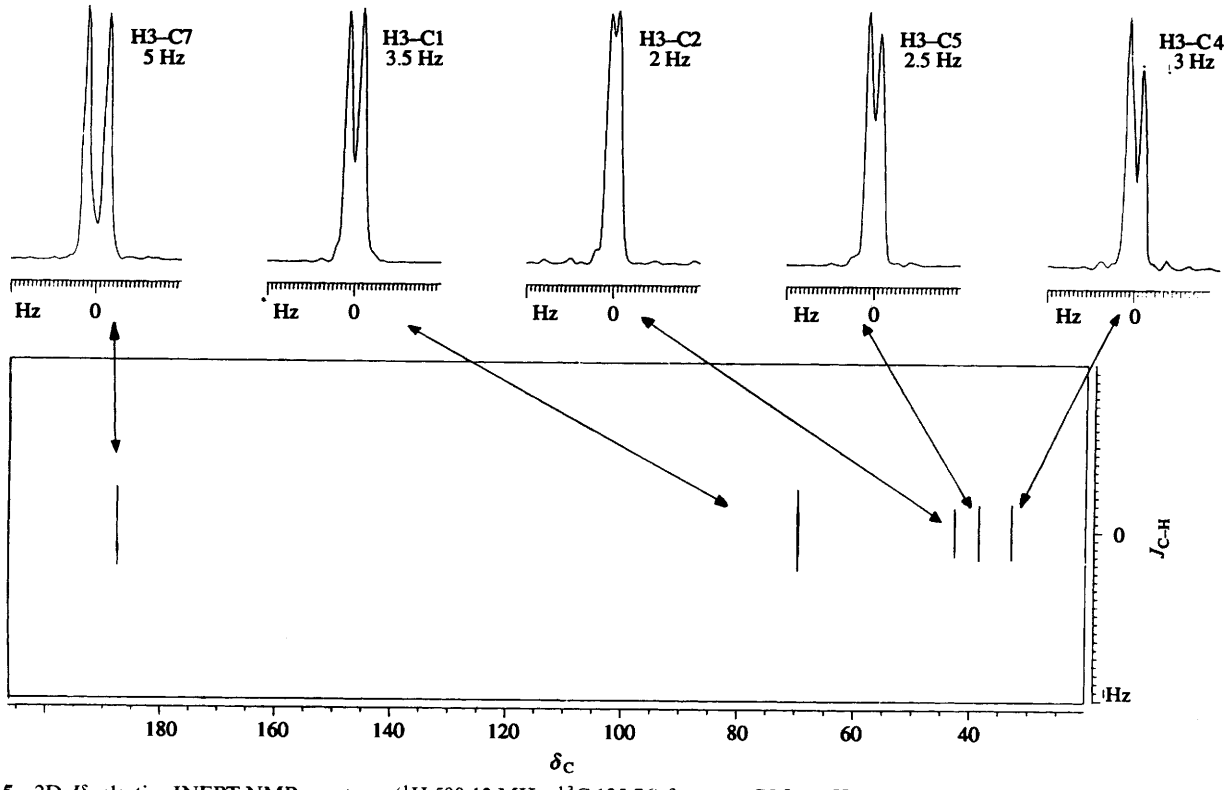

Fig. 5 2D *Jδ* selective INEPT NMR spectrum (^{1}H 500.13 MHz, ^{13}C 125.76) for *trans*-C5 **2** at pH 7

The measurement of heteronuclear long-range $^3J_{^{13}C-^1H}$ coupling constants (Table 3) combined with MD studies (Table 4) were also useful to identify the mobility of the ring moiety and the positions of the substituents with respect to the cyclopentane. It is of particular interest since it could be related to the different biological properties of this molecule. Values of the coupling constants obtained from selective 2D INEPT[23] are given in Table 3 for $^3J_{H(3)C(1)}$ and $^3J_{H(3)C(5)}$. The measured values of $^3J_{CH}$ for **1** **2**, are $^3J_{H(3)C(1)}$ and $^3J_{H(3)C(5)} \leq 1$ Hz. They characterize conformations with φ[H(3b)–C(3)–C(4)–C(5)] =

Table 4 Energy, torsion angles and calculated[a] coupling constants (^3J/Hz) computed for **1**, from different conformations generated by MD at different protonation states; H noted a or b according to the geometrical isomerism of the proton (Ha and NH_3^+ *trans*; Hb and NH_3^+ *cis*)

	cis-C5 **1**				
	1 2 ^2E	**1 2** $^2T_3 = E_3$	**1 1** ^2E	**1 1** E_5	**1 3** ^2E
E_p/kcal mol^{-1}	4.9	7.8–8.7	6.9	7.8	31.6
φ(°)(^3J/Hz) 3b, 2a	−167.0	−171.3	−169.7	−113.7	−165.9
	(12.6)	(12.9)	(12.8)	(2.6)	(12.5)
3b, 2b	−48.6	−55.4	−51.3	1.7	−47.4
	(5.2)	(3.9)	(4.7)	(11.7)	(5.5)
3b, 4a	147.7	167.6	156.2	148.38	145.8
	(9.7)	(12.6)	(11.2)	(9.8)	(9.3)
3b, 4b	28.6	48.0	36.8	27.8	26.6
	(8.9)	(5.3)	(7.3)	(9.0)	(9.3)
4a, 5a	7.4	−27.4	−5.4	−42.6	9.8
	(11.6)	(9.4)	(11.8)	(6.5)	(11.5)
4a, 5b	−108.3	−141.9	−120.5	−160.8	−106.2
	(1.7)	(8.4)	(3.7)	(11.9)	(1.4)
4b, 5a	125.0	91.3	12.0	75.9	127.4
	(4.9)	(0.3)	(2.4)	(0.8)	(5.4)
4b, 5b	9.3	−23.1	−3.2	−42.2	11.5
	(11.5)	(10.0)	(11.8)	(6.5)	(11.4)
3b-H, C-1	75.0	70.2	72.3	−120.6	75.9
	(0.7)	(0.9)	(0.8)	(2.3)	(0.7)
3b-H, C-5	−92.9	−74.1	−85.4	−94.0	−94.5
	(0.6)	(0.8)	(0.5)	(0.6)	(0.6)

[a] The coupling constants values $^3J_{HH}$ calculated by Altona's equations[24] and the $^3J_{CH}$ values by a Karplus type-equation:[25] $^3J_{CH} = 5.7\cos^2\varphi - 0.6\cos\varphi + 0.5$.

Table 5 Energy, torsion angles and calculated coupling constants[a] (^3J/Hz) computed for **2**, from different conformations generated by MD at different protonation states; H noted a or b according to the geometrical isomerism of the proton (Ha and NH_3^+ *trans*; Hb and NH_3^+ *cis*)

	trans-C5 **2**							
	2 2 $^2T_1 = E_1$	**2 2–2 1** $^5T_1 = {}^5E$	**2 2–2 3** $^5T_4 = E_4$ (X-ray)	**2 2–2 1** $^3T_4 = {}^3E$	**2 2–2 1** $^3T_2 = E_2$	**2 2–2 3** $^1T_2 = {}^1E$	**2 2** $^4T_5 = {}^4E$	**2 2** E_3
E_p/kcal mol^{-1}	—	6.2–7.1[b]	32.4[b]	6.8[b]	6.9[b]	32.7[b]	—	—
	1.4[c]	5.1–5.3[d]	6.9–7.1[d]	7.6–8.3[d]	12.5–14.5[d]	10.1–11.9[d]	6.8[d]	9.9[d]
φ(°)(^3J/Hz) 3a, 2a	−24.1	8.4	30.0	52.7	44.4	41.0	49.8	−33.1
	(9.8)	(11.5)	(8.9)	(4.4)	(6.0)	(6.6)	(4.9)	(7.6)
3a, 2b	91.5	122.6	147.3	169.3	162.7	158.9	165.8	82.4
	(0.4)	(4.2)	(9.5)	(12.8)	(12.2)	(11.7)	(12.5)	(1.7)
3a, 4a	−4.6	−32.8	−46.9	−51	−17.9	−12.2	−51.5	29.6
	(11.5)	(8.2)	(5.5)	(4.6)	(10.5)	(11.9)	(4.6)	(8.1)
3a, 4b	−123.4	−152.7	−167.8	−171.5	−137.1	−131.5	−172.8	−88.7
	(4.3)	(10.3)	(12.5)	(12.9)	(7.5)	(6.3)	(12.9)	(1.4)
4a, 5a	26.0	41.9	44.2	32.2	−22.2	−27.1	36.3	−23.4
	(9.6)	(6.5)	(6.6)	(8.5)	(10.2)	(9.4)	(7.3)	(8.8)
4a, 5b	−90.7	−76.0	−72.9	−83.1	−138.4	−143.7	−79.3	−138.2
	(0.4)	(0.9)	(1.2)	(0.5)	(7.9)	(9.1)	(0.6)	(4.9)
4b, 5a	143.3	161.2	164.8	151.9	95.3	90.6	156.2	93.9
	(8.6)	(11.9)	(12.4)	(10.4)	(0.5)	(0.4)	(11.4)	(1.3)
4b, 5b	26.7	43.3	47.8	36.6	−21.0	−25.9	40.6	−20.9
	(9.5)	(6.3)	(5.4)	(7.7)	(10.4)	(9.6)	(6.8)	(9.1)
3a-H, C-1	−141.6	−110.9	−89.1	−70.8	−78.8	−82.7	−74.4	−150.8
	(4.5)	(1.5)	(0.5)	(0.9)	(0.6)	(0.5)	(0.8)	(5.3)
3b-H, C-5	116.6	88.6	73.6	70.0	101.8	107.0	68.9	146.9
	(2.0)	(0.5)	(0.8)	(0.9)	(0.9)	(1.2)	(1.0)	(5.0)

[a] The coupling constants values $^3J_{HH}$ would be calculated by Altona's equations[24] and the $^3J_{CH}$ values by a Karplus type-equation:[25] $^3J_{CH} = 5.7\cos^2\varphi - 0.6\cos\varphi + 0.5$. [b] Potential energies of the structures generated by the first protocol with a selected value of the relative permittivity ($\varepsilon = 5$) for *trans*-C5 **2** at various pH values (**2 1** and **2 3**). [c] The potential energy of this structure **2 2** generated by the second protocol in a solvation box is 3.7 kcal mol^{-1}. [d] Potential energies of the structures **2 2** generated by the second protocol in a solvation box. The molecules are minimized by a single iteration of the steepest descent algorithm, after removing water molecules.

± 90° as torsion angles and this implies that the orientation of 3b-H with respect to the five membered ring is almost the same whatever the conformation of the isomer **1 2** is: 3b-H axial, γ- and α-CO_2^- groups diequatorial, α-NH_3^+ axial (Fig. 6). The torsion angles of structures generated by MD, can be correlated by using a Karplus type-equation[25] to the corresponding coupling constants. Thus, the data show approximately similar values to those predicted for **1 2** ^2E, **1 2** $^2T_3$ or **1 2** E_3.

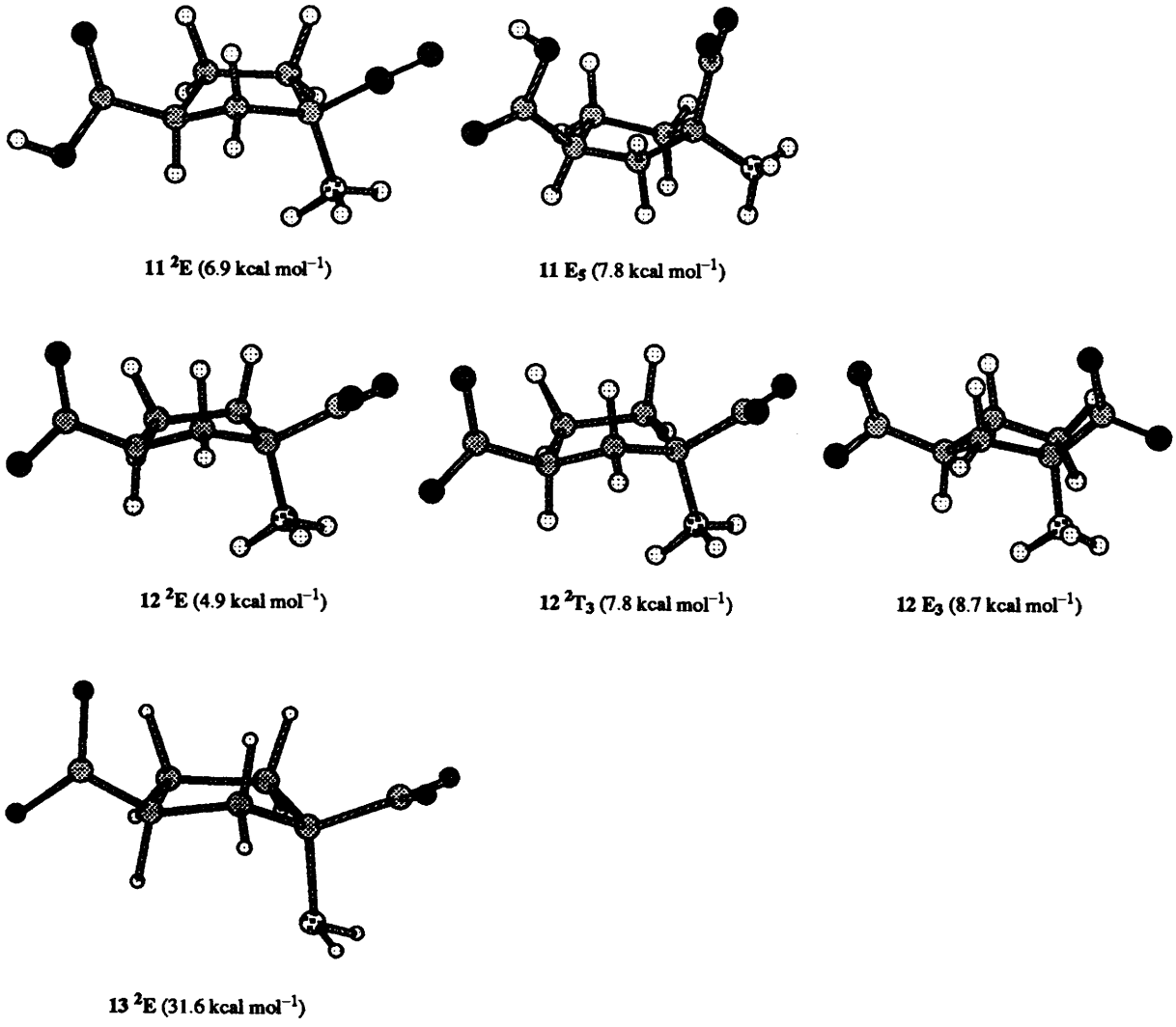

Fig. 6 Stable structures generated by the first protocol with a selected value of the relative permittivity (ε = 5) for *cis*-C5 **1** at various pH values and achieved conformations for *cis*-C5 **1** at pH 7 by MD with water molecules; potential energies of the system (C5 + 18H_2O) and in parentheses, the energies of the corresponding C5 molecules, minimized by a single iteration of the steepest descent algorithm, after removing water molecules: ^{2}**E** E_p = −126.2 (7.7); ^{2}**T**$_3$ E_p = −126.0 (7.8); **E**$_3$ E_p = −118.3 (8.7) kcal mol^{-1}

***trans*-C5 2.** For this isomer, coupling constants are deduced from 1D spectra at 500 MHz, and confirmed by spectral simulation. In addition, homodecoupling experiments are employed. In the *trans*-isomer $^3J_{trans}$ is smaller than $^3J_{cis}$ at two different pH values. At pH 7.0, 3a-H presents *trans*-oriented coupling $^3J_{HH}$, $^3J_{3a,2b}$ and $^3J_{3a,4b}$ ($\approx$ 5 Hz) being smaller than *cis*-oriented coupling, $^3J_{3a,2a}$ and $^3J_{3a,4a}$ (8.5 Hz). This inversion indicates a change in the conformation of the substituted cyclopentane. In this privileged conformation, 3a-H is in an isoclinal position, more weakly coupled with its neighbouring *trans* protons and found nearly eclipsing 2a- and 4a-H (large coupling). In the *trans*-series an increase of the axial character of the γ-CO_2^- and α-NH_3^+ groups is observed, the ammonium group displaying a more axial character than the 3-carboxylate. The analysis of the spin-system was confirmed by spectral simulation (Fig. 4). At pH 3.0, the mentioned coupling constants are averaged ($^3J_{3a,2b}$ and $^3J_{3a,4b}$ $\approx$ 7 Hz), thus the molecule is in conformational equilibrium with a conformer in which 3a-H is axial (equatorial γ-CO_2H group on C-3). At pH 11.0, the equilibrium still exists but the latter conformer, axial 3a-H, equatorial γ-CO_2H is now predominant. The 3a-H signal is in agreement with an axial proton coupled to two axial neighbours 2b- and 4b-H ($^3J_{3a,2b}$ and $^3J_{3a,4b}$ $\approx$ 10.0 Hz). Therefore, at extreme pH (3.0 and 11.0), the preferred conformations are the sterically favoured ones (axial 3a-H, equatorial γ-CO_2^-). While at intermediate pH (7.0), the conformer (isoclinal 3a-H, axial γ-CO_2^-) is very probably stabilized by an electrostatic interaction (analogous to a hydrogen bond) between the 1-ammonium (α-NH_3^+) and the 3-carboxylate group (γ-CO_2^-).

For the *trans*-C5 isomer **2 1** (at isoelectric pH), we have reported in Table 3 the coupling constants from NMR spectra, and those calculated by Altona's equation [24] from the X-ray structure **2 1 E**$_4$ or **2 1** ^{5}**T**$_4$ (shown in Fig. 3), with equatorial γ-CO_2H, isoclinal α-CO_2^- and α-NH_3^+. The experimental values for compound **2 1** are not in good agreement with the calculated values for **2 1 E**$_4$.

Determination of heteronuclear ^{13}C–^{1}H coupling constants by the selective 2D INEPT experiment [23] is especially helpful for 3a-H bonds in order to determine the relative positions of the substituents on the five-membered ring (Fig. 5). The selective excitation of 3a-H for H(3)C(3)C(2)C(1) and for H(3)C(3)-C(4)C(5), led to the $^3J_{CH}$ values presented in Table 3. The data $^3J_{H(3a)C(1)}$ = 3.5 and $^3J_{C(5)H(3a)}$ = 2.5 Hz, support a predominant conformation for the substituted ring but a conformational averaging could also give good agreement with experimental NMR data. Our observed values can be compared to those of

Table 6 Longitudinal relaxation times (T_1/s) for ^{13}C in D_2O at pH 7 (error of 5%)

C	*cis*-C5 **1 2** $T_1(NT_1)$	*trans*-C5 **2 2** $T_1(NT_1)$	$\Delta NT_1 \times 100/NT_1$ *cis*
2 CH_2	0.62	0.9	
	(1.24)	(1.8)	+45%
3 CH	1.28	1.67	+30%
4 CH_2	0.99	1.18	
	(1.98)	(2.36)	+20%
5 CH_2	0.82	1.06	
	(1.64)	(2.12)	+30%

minimized structures (Table 5), generated by MD study *versus* the different protocols (Fig. 7): for the isomer **2 2**, $^3J_{H(3)C(1)}$ = 3.5 and $^3J_{C(5)H(3)}$ = 2.5 Hz should include a large participation of conformer **2 2 E**$_1$ ($^3J_{H(3)C(1)}$ = 4.5 and $^3J_{H(3)C(5)}$ = 2.5 Hz).

^{13}C longitudinal relaxation times (T_1). Information about the structural flexibility of these compounds can be obtained experimentally from the T_1 relaxation times of the carbon resonances. The NT_1 values (N = number of attached protons, T_1 = longitudinal relaxation time) correlate directly with the molecular mobility. This is due to the fact that the ^{13}C relaxation of these carbons is mainly dominated by the single relaxation mechanism, that is, ^{13}C–^1H dipolar interaction with directly bonded hydrogens.[26]

The NT_1 values measured by inversion-recovery experiments at pH 7.0 are reported in Table 6. These data provide us with information about rotational motion of the backbone of glutamic acid derivatives and about the internal rotations of the substituents. All the carbons gave similar NT_1 values, indicating some rigidity of the backbone. For each of the carbons, NT_1 values are larger in the *trans*-isomer **2** than in the *cis*-isomer **1**. These results showed that the *trans*-C5 **2** ring is more mobile than the *cis*-C5 unit. Fig. 8(*a*) displays for **2**, differences for the amplitudes of the endocyclic torsion angles C(1)–C(2) and C(2)–C(3) (≈80°) in the *trans*-C5 moiety, during 100 ps simulation, with respect to the same region in the *cis*-C5 isomer. The smaller T_1 values for the *cis*-C5 ring were indicative of sterically hindered mobility. The low amplitude (≈10°) of endocyclic torsion angles C(1)–C(2) and C(2)–C(3) in the C5-ring region is observed during the MD of the *cis*-C5 isomer, even in the protocol with temperature jumps to 600 K [Fig. 8(*b*)].

Molecular dynamics

We performed computational chemical methods (molecular dynamics and molecular mechanics calculations), starting with the X-ray crystal structure of the *trans*-C5 **2**. The final structures obtained after several such calculations were examined for the overall energetic favourability and compared with the structure derived from the NMR data. The aims of this work are to use molecular dynamics calculations (*i*) to determine the flexibility of the carboxylate or ammonium groups about the bonds joining these substituents to the cyclopentane ring and predict the available conformational space for active groups and (*ii*) to determine the pseudorotation about the endocyclic torsion angles in the cyclopentane and thus, to generate the approximate ratios of minimum-energy conformations available up to 1–3 kcal mol^{-1}. The structures found to have more energy, up to 10 kcal mol^{-1} will be representative of very hindered intermediates.† Tables 4 and 5 present the resulting dihedral angles for all different conformations obtained from MD.

The similarity between the geometry in solution and several MD conformers is investigated from the 100 minimized structures generated. The torsion angles of generated structures can be correlated to the corresponding coupling constants by using Karplus-type equations.[24,25] Tables S1 and S2 (of supplementary material)‡ sum the exploration of conformational space covered during the simulations (potential energy and evolution of endocyclic torsion angles around cyclopentane ring). They allowed us to analyse the different substituent positions (axial or equatorial orientation).

Preliminary protocols. MD simulations were carried out using the DISCOVER and INSIGHTII programs from the BIOSYM package[27] on a Silicon-Graphics computer. We performed the MD calculations starting with X-ray structures of the *trans*-C5 **2**, without applying the distance or the dihedral angles' constraints obtained from the NMR experiments.

The X-ray structure of the *trans*-C5 **2**, were used to build the molecular structure and topology for **2 1**, **2 2**, **2 3** respectively, with replacement of the carboxy group by a carboxylate for the unprotonated derivatives **2 2** and **2 3** and with the protonated amino group modified to an amine for **2 3**. The starting coordinates of the *trans*-C5 **2**, are used as the starting conformation for the simulation of **1**, with the opposite configuration of the 3-carboxylate group.

The technique used to generate the structures include an empirical method to simulate the molecular movements in solution and to verify if the sampling of the conformational space is almost complete during the MD calculations. For a preliminary exploration of the conformational space, after energy minimization and an equilibration period of 4 ps, we performed for **1 1**–**1 3** and **2 1**–**2 3** a 50 ps MD run at 300 K with periodic temperature jumps to 600 K to supply the system with energy (to pass conformational barriers). The 50 ps trajectory was sampled every picosecond and the remaining structures were then minimized by molecular mechanics and stored.

The available low-energy conformers were also reproduced after the modelling procedure starting from each one of the possible conformations to compare their energies in the interconversion. The stability of the different conformers of *cis*-C5 **1** and *trans*-C5 **2** was tested at different pH by a protocol without raising the temperature (300 K) but using a long time scale (100 ps) with energy minimization every 1 ps.

Particular attention had to be given to the modelling of electrostatic interactions (including hydrogen bonding), which were calculated in the force field by a coulombic expression.

Protocol I.—[With the relative permittivity (dielectric constant) adjusted as in previous studies.][12] A widely used method to mimic the solvent's screening effect is to use a distance-dependent relative permittivity $\varepsilon = r$, leading to an r^2 dependence of the coulombic energy.[28] In a previous study,[12] these experiments with $\varepsilon = r$, allowed us to confirm some of the results obtained by NMR spectroscopy, but the force field seemed unsuitable to characterize the 1,3-diaxial electrostatic interactions and thus, had to be modified. Use of a distance-dependent relative permittivity ($\varepsilon = r$) in the absence of explicit solvent is common, but it is a crude approximation to reality and it cannot deal properly with strong charge interactions such as occur in these molecules. Hence the behaviour of the calculations under this protocol was not unexpected. It is possible to model explicitly the solvent effect in the vicinity of the molecules: we used the electrostatic interaction expression $E = K \times q_1q_2/\varepsilon r$ and tried to adjust the relative permittivity to a value, between 1 and 78.54,[28] corresponding to the interactions in aqueous solution.

† 1 cal = 4.184 J.

‡ For details of the supplementary publications scheme, see 'Instructions for Authors (1995)', *J. Chem. Soc., Perkin Trans. 2*, 1995, issue 1 [Supp. Pub. No. 57081 (4 pp.)].

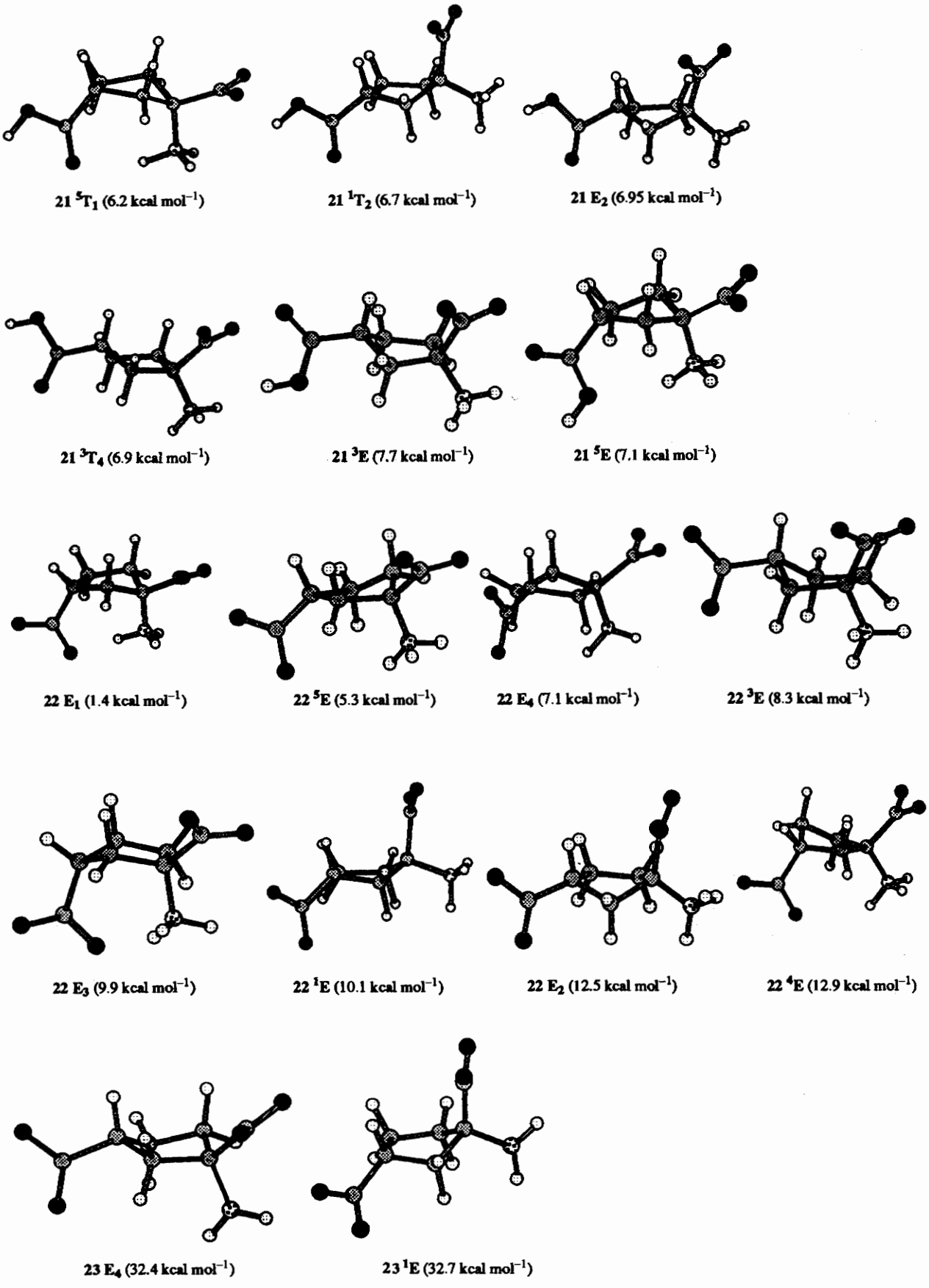

Fig. 7 Stable structures generated by the first protocol with a selected value of the relative permittivity (ε = 5) for *trans*-C5 **2** at various pH values; achieved conformations for *trans*-C5 **2** at pH 7 by MD with water molecules and only the forms, envelope **E** are represented; potential energies of the system (C5 + 18H_2O or C5 + 22H_2O) and in parentheses, the energies of the corresponding C5 molecules, minimized by a single iteration of the steepest descent algorithm, after removing water molecules: $\mathbf{E}_1$ E_p = −264.8 (3.7); $^5\mathbf{E}$ E_p = −260.9 (5.3); $\mathbf{E}_4$ E_p = −258.6 (6.9); $^3\mathbf{E}$ E_p = −257.4 (8.3) kcal mol^{-1}; $\mathbf{E}_2$ E_p = −254.2 (12.0); $^1\mathbf{E}$ E_p = −257.6 (10.1); $^4\mathbf{E}$ E_p = −248.2 (12.9); $\mathbf{E}_3$ E_p = −248.1 (9.9) kcal mol^{-1}

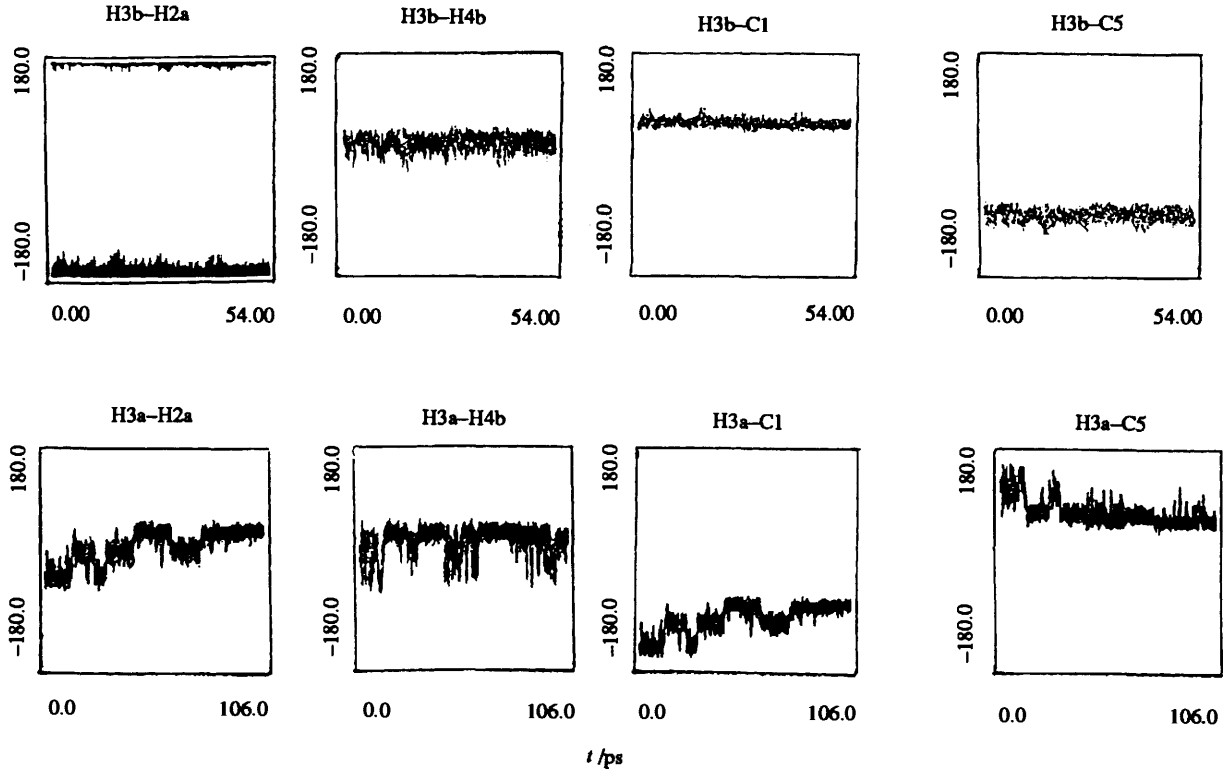

Fig. 8 (*a*) Trajectories of some characteristic homonuclear dihedral angles and heteronuclear dihedral angles for *trans*-C5 **2** at pH 7 by MD with water molecules at 300 K (top). The atoms in the *trans*-C5 **2** isomer are relatively more mobile than the atoms in the *cis*-C5 **1** isomer even during simulation at 300 K; (*b*) trajectories of some characteristic homonuclear dihedral angles and heteronuclear dihedral angles for *cis*-C5 **1** at pH 7 by MD with water molecules at 600 K (bottom). The flexibility is hindered, even with temperature jumps during the MD.

We used the results of the NMR experiments on the conformational equilibrium observed for the *trans*-C6 at pH 4.0 and 7.0. We performed dynamics starting from each one of the possible chairs for this isomer, with different values of ε and correct energy differences between the two chairs' forms are obtained for $\varepsilon = 5$. With this value of the relative permittivity, experiments were run starting from each of the possible conformers for the two isomers. The results are summarized in Figs. 6 and 7.

Protocol II.—It is possible to mimic the solvent effect with explicit modelling of water: we have constructed solvation boxes containing the C5 molecule and several water molecules using periodic boundary conditions (Fig. 9). The relative permittivity was set to $\varepsilon = 1$. Experiments were carried out on the forms **1 2** and **2 2** of *cis*-C5 **1** and *trans*-C5 **2**. The different minimized structures and their energies are reported in Figs. 6 and 7. The results are consistent with the two protocols, but electrostatic interactions do not stabilize the lowest-energy conformer as much as in the first protocol where they may be overestimated.

This second protocol is not of practical use: the CPU times are much longer (24 h) than for a single molecule (0.5 h), and the energies obtained are those of C5 + $18H_2O$ systems; thus the energies of the corresponding minimized C5 molecules themselves are very difficult to evaluate. The minimization consisted of a single iteration of the steepest descent algorithm in order to measure the potential energy for each structure, after removing water molecules. Therefore, we conceived that the first protocol avoiding the introduction of explicit water molecules would rapidly give results in conformational studies on other glutamic acid derivatives for conformational systematic searches or for simulated-annealing.

***cis*-C5 1**. At each pH, the energies of all conformers were compared (Fig. 6). At pH 7 the ^{2}**E** envelope conformation, predominant in solution according to NMR results, has an energy about 3 kcal lower than that of the half-chair ^{2}**T**$_3$. It should be noticed that in these two conformations, the two carboxylate groups are lying equatorial. At alkaline pH, no interconversion was observed, ^{2}**E** being the single conformer identified. However, at isoelectric pH, an electrostatic attraction between the 3-carboxy and the 1-carboxylate axial groups, led to an interconversion to **E**$_5$. The **E**$_5$ and ^{2}**E** conformers have

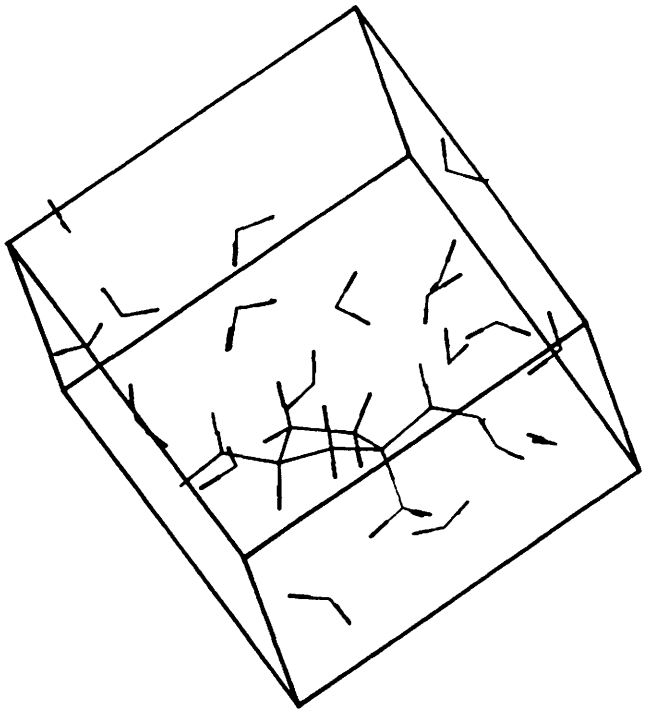

Fig. 9 Solvation box containing the C5 molecule and several water molecules (*cis*-C5 + $18H_2O$) to mimic the solvent effect with explicit modelling of water in molecular dynamics protocol **II**

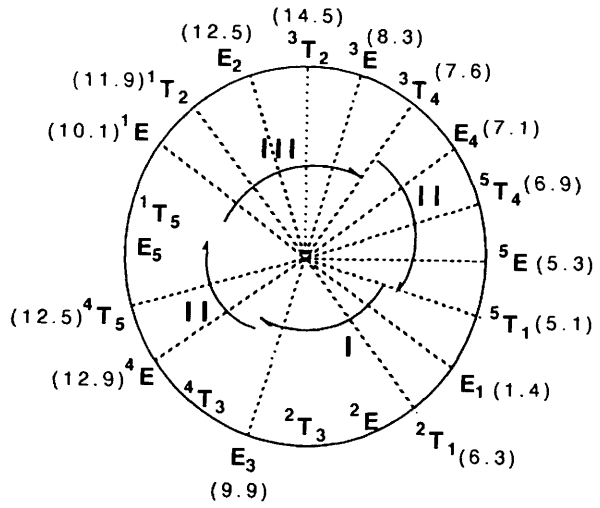

Fig. 10 Pseudorotational pathway of the *trans*-C5 **2 2** ring at pH 7 with the presence of a different number of water molecules. Each external point of dotted radials in the circle represents a specific **E** form or **T** conformation generated by all the different MD experiments. Heavy arrows indicate the corresponding family type.

energies in the same range, ^{2}**E** conformer being more stable. This is coherent with the NMR results (Tables 3 and 4) confirming the observed averaged coupling constants in solution (see $^3J_{3.2a}$ and $^3J_{3.2b}$). This $\mathbf{E}_5$ structure was never generated at pH 7, whatever the protocol or the temperature. It was important to verify if this 'folded' structure $\mathbf{E}_5$ would be representative of a hindered intermediate for this isomer, at neutral pH. Therefore, to create this same starting structure $\mathbf{E}_5$ for *cis*-C5 **1 2** at pH 7, we have chosen to force the torsions C(6)C(1)–C(2)C(3) and C(7)C(3)–C(2)C(1) to the values found for **1 1** $\mathbf{E}_5$ in the previous experiment, 93° and −120° respectively, while all other torsions were not forced. These values were then introduced using a relatively high force constant of 35 kcal mol^{-1} (15 kcal mol^{-1} has proved to be too low), and the system was allowed to come to equilibrium for 4 ps. This structure was not stable during the protocol and the **1 2** $\mathbf{E}_5$ form was transformed into the **1 2** ^{2}**E** conformer at the beginning of the dynamics. This experiment aborts, the $\mathbf{E}_5$ conformation probably being destabilized by an overestimated electrostatic repulsion between the two 1,3-diaxial carboxylate groups.

We have run dynamics under the second protocol with explicit water molecules. At the considered pH, the lower-energy **1 2** ^{2}**E** conformer was stable, confirming the results of the first protocol. All the dihedral angles measured varied less than 10° during the dynamics (Fig. 8), except for the oxygen atoms exchanging their positions into the α- and γ-carboxylate groups by 180° rotation. At neutral pH, the **1 2** ^{2}**E** conformer led to a less stable conformer **1 2** $\mathbf{E}_3$ *via* a twist intermediate $^2\mathbf{T}_3$ but interconversion to **1 2** ^{5}**E** was not observed (Fig. 6, Table 4). At pH 7, the two carboxylate groups always adopted an equatorial and the amino group an axial position, whatever the conformation. This is coherent with the NMR results (Table 3), confirming that the **1 2** ^{2}**E** conformer was the preponderant one in solution at any pH.

***trans*-C5 2.** At pH 7, no interconversion was observed with the first protocol. The $\mathbf{E}_1$ structure was stable during the whole protocol while the X-ray $\mathbf{E}_4$ or $^5\mathbf{T}_4$ forms were transformed into the $\mathbf{E}_1$ conformer at the beginning of the dynamics. In the *trans*-isomer **2**, a 1,3-diaxial electrostatic attraction stablizes the **2 2** $\mathbf{E}_1$ conformer with the α-NH_3^+ and γ-CO_2^- in an axial (or isoclinal) position. This was coherent with the NMR results, confirming that the **2 2** $\mathbf{E}_1$ conformer was the preponderant one in solution, but the data did not support a single conformation model for the ring and only conformational averaging could give good agreement between theoretical (MD) and experimental (NMR) data. In the absence of explicit water molecules, an overestimated electrostatic attraction between the 1-ammonium and the 3-carboxylate led to a single stable conformer.

To locate other stable contributing conformations, the 48 ps trajectory (at 300 K, with periodic temperature jump to 600 K) was sampled every picosecond in a water box. In that case, an interconversion was observed, at neutral pH where the $\mathbf{E}_1$ conformer led to the less stable conformer ^{5}**E** (Fig. 7) *via* a twist intermediate $^5\mathbf{T}_1$. Therefore, at pH 7, γ-CO_2^- and α-NH_3^+ stayed respectively in a 'folded' position (isoclinal–axial) stabilized by the 1,3-electrostatic attraction (or axial–isoclinal only for two high energy structures: one ^{4}**E** and one $\mathbf{E}_3$), whatever the possible isomer was. The preferred conformation was the favoured $\mathbf{E}_1$. This experiment allowed us to confirm some of the results obtained by NMR spectroscopy. For example, determination of heteronuclear ^{13}C–^{1}H coupling constants by the selective 2D INEPT experiment was especially helpful in order to investigate the position of the γ-carboxylate group relative to the C5-ring by the selective excitation of the ring H-3 (Fig. 5). Our observed values for $^3J_{C(1)H(3)}$ (3.5 Hz) and $^3J_{C(5)H(3)}$ (2.5 Hz) could be compared to those of minimized structures (Table 5), generated by MD studies *versus* the different protocols (Fig. 7). The orientation of the γ-carboxylate group with respect to the ring was different for both conformers and these values should include a larger participation of conformer **2 2** $\mathbf{E}_1$ ($^3J_{H(3)C(1)}$ = 4.5 Hz and $^3J_{H(3)C(5)}$ = 2.0 Hz) than **2 2** ^{5}**E** ($^3J_{H(3)C(1)}$ = 1.5 Hz and $^3J_{H(3)C(5)}$ = 0.5 Hz). The **2 2** $\mathbf{E}_1$ conformer is very probably stabilized by an electrostatic interaction (similar to a hydrogen bond) between the 1-ammonium and the 3-carboxylate groups.

Conformations of 'higher energy' with γ-CO_2^- and α-NH_3^+ in an equatorial–isoclinal position (4 and 10 kcal above the minimum) were also generated for **2**: ^{3}**E** and the X-ray $\mathbf{E}_4$ (Fig. 7) in a box filled with 18 water molecules and $\mathbf{E}_2$ and ^{1}**E** (Fig. 7) in a box with 22 water molecules. These structures would participate to a small extent ($^3J_{H(3)C(1)}$ = 0.5–0.9 Hz and $^3J_{H(3)C(5)}$ = 0.8–0.9 Hz) in *trans*-C5 **2** conformation. They are stabilized by an aqueous environment. The energy of the corresponding minimized structures can be evaluated after the removal of the water molecules, only if the relative permittivity was set to ε = 60–78. Fig. 10 shows the successive conformations (**E** or **T** forms) on the pseudorotational cycle, during all the MD experiments.

At pH 3 and 11, the electrostatic interactions are minor and the isomers with lowest energies have the equatorial groups according to the NMR results. Several conformations are sterically favoured (Fig. 7). At alkaline pH, a conformational equilibrium between conformers $\mathbf{E}_4$ and ^{1}**E** occurs with γ-CO_2^- and α-NH_2 equatorial or isoclinal, and α-CO_2^- isoclinal or axial, confirming the results of NMR experiment (Tables 3 and 5). At isoelectric pH, six conformers have energies in the same range and only conformational averaging can give good agreement between theoretical (MD) and experimental NMR data (Tables 3 and 5). At this intermediate pH (4.0), $^5\mathbf{T}_1$ and ^{5}**E** with γ-CO_2H and α-NH_3^+ respectively in isoclinal–axial position are stabilized by the same type of electrostatic interaction between the 1-ammonium and the 3-carboxy groups. At this pH (4.0), the other isomers have 3-H axial and two equatorial or isoclinal groups: $^1\mathbf{T}_2$ and $\mathbf{E}_2$ have two equatorial groups (γ-CO_2H and α-NH_3^+) and α-CO_2^- axial while $^3\mathbf{T}_4$ and ^{3}**E** have two isoclinal groups (α-CO_2^- and α-NH_3^+) and one equatorial (γ-CO_2H). The coupling constants for 3-H were calculated from the dihedral angles of each conformer generated by MD. An average of 3-H axial and 3-H equatorial is in good agreement with the coupling constants obtained from NMR spectra (Tables 3 and 5).

The most significant dihedral angles of the minima for **2**

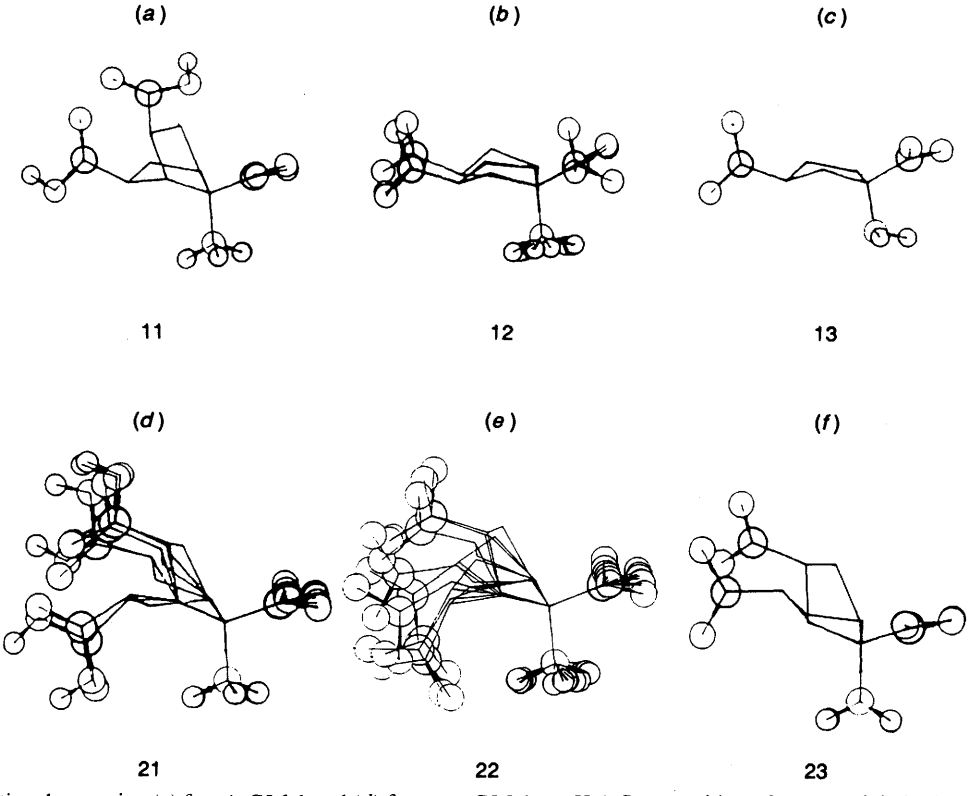

Fig. 11 Conformational averaging (*a*) for *cis*-C5 **1 1** and (*d*) for *trans*-C5 **2 1** at pH 4. Superposition of energy minimized structures **1 1** (^{2}**E**, **E**$_5$) and **2 1** (^{5}**T**$_1$, ^{5}**E**, ^{1}**T**$_2$, **E**$_2$, ^{3}**T**$_4$, ^{3}**E**) computed by MD calculations with the first protocol ($\varepsilon = 5$), corresponding to the two families **II** and **IV** for **1 1** and **I** and **III** for **2 1**; conformational averaging (*b*) for *cis*-C5 **1 2** and (*e*) for *trans*-C5 **2 2** at pH 7. Superposition of energy minimized structures **1 2** (^{2}**E**, ^{2}**T**$_3$, **E**$_3$) and **2 2** (**E**$_1$, ^{5}**E**, **E**$_4$, ^{3}**E**, **E**$_2$, ^{1}**E**, ^{4}**E**, **E**$_3$; and **T** forms have been removed for clarity) computed by MD calculations with water molecules at 300 K, corresponding to the family **II** for **1 2** and to the three families **I**, **II** and **III** for **2 2**; conformational averaging (*c*) for *cis*-C5 **1 3** and (*f*) for *trans*-C5 **2 3** at pH 11. Energy minimized structure **1 3** (^{2}**E**) and (**E**$_4$, ^{1}**E**) computed by MD calculations with the first protocol ($\varepsilon = 5$), corresponding to the family **II** for **1 3** and to the two families **II** and **III** for **2 3**. Hydrogens have been removed for clarity.

were measured and compared with the values for the crystalline structure **2 1** (Table S2 of the supplementary material): obviously, the values for only one conformer of **2 2** and **2 3** (**E**$_4$) are very close to the X-ray data, while the conformations for **2 1** are totally different.

The first protocol, in which one experimental result is used to select a value of the relative permittivity so as to make calculations agree with experiment, is the preferred choice for a preliminary systematic search. It is understood that such a choice has little or no physical meaning and will be applicable only to a limited range of structures. For the other molecules, a protocol with explicit modelling of water is the preferred choice and in this case, the appropriate value of the relative permittivity is 1.

From the various solutions resulting from the MD approach, one set presented best minimized intramolecular energy and good agreement with the coupling constants obtained from NMR spectra; *i.e.* vicinal $^3J_{^1H,^1H}$ coupling constants and especially, long-range heteronuclear ^{13}C, ^{1}H coupling constants determined by the selective 2D INEPT experiment.

Structural characteristics of ACPD ligands. The superimposition of C(1) and of the central atoms of the two functional groups (see numbering in Fig. 3), *i.e.*, the α-N(1) and α-C(6) (α-CO_2^-) of the different conformers deduced from the NMR and MD data of the two isomers analogues *cis*- and *trans*-ACPD (Fig. 11) displays four conformational families **I**–**IV**. The different families are characterized by physical features of the potentially active functional groups (Fig. 12 and Table S3 of the supplementary material), such as the distances (Å) d_1 [d(α-NH_3^+ –γ-CO_2^-)] and d_2 [d(α-CO_2^-–γ-CO_2^-)]. The quality of the superimposition of the three central atoms was evaluated by the root mean square (rms) deviation between the atoms constituting the major conformer in the molecule and the corresponding atoms in the other conformations.

The differentiation of the four families is due to the electrostatic attraction or repulsion along with the steric hindrance. The type **I** [Fig. 12(*a*)] displays an attractive electrostatic potential between the α-NH_3^+ and γ-CO_2^- groups and thus, the shortest distance d_1 between these two functional groups. It can only be found in the case of the *trans*-ACPD isomer when the two groups have two opposite charges at neutral pH. The distance d_2 has an intermediate value. The type **II** [Fig. 12(*b*)] is characterized by the greatest distance d_2 between the functional groups with the same charges α-CO_2^- and γ-CO_2^-. The predominant conformation of the *cis*-ACPD isomer **1** belongs to this type. Meanwhile the distance d_1 remains relatively small, thus the minor conformers (at pH 7) of the *trans*-ACPD isomer **2** also belong to this family. The type **III** [Fig. 12(*c*)] is characterized by a relatively short distance d_2 and a relatively long distance d_1. The 'higher energy' structures at pH 7 of *trans*-ACPD **2** are of this type. But these structures become more stable at pH 3, since the protonation of the γ-carboxyl group creates hydrogen bonding with α-CO_2^-. It results in a close proximity of the two groups. Finally, the type **IV** [Fig. 12(*d*)] is characterized by the shortest distance d_2 between the two carboxyl groups. It is only found at pH 4 for the *cis*-ACPD **1**, when the γ-carboxyl group is protonated.

As compared to the parent molecules, these flexible compounds C5 **1** and **2** have a good structural analogy with the rigid C6 analogues. The *cis*- and *trans*-C5 ligands provide a useful tool to explore the structural and functional relationships between ligands belonging to different classes of molecules [Fig. 12(*e*)], in biological systems (NMDA or ACPD receptors of the

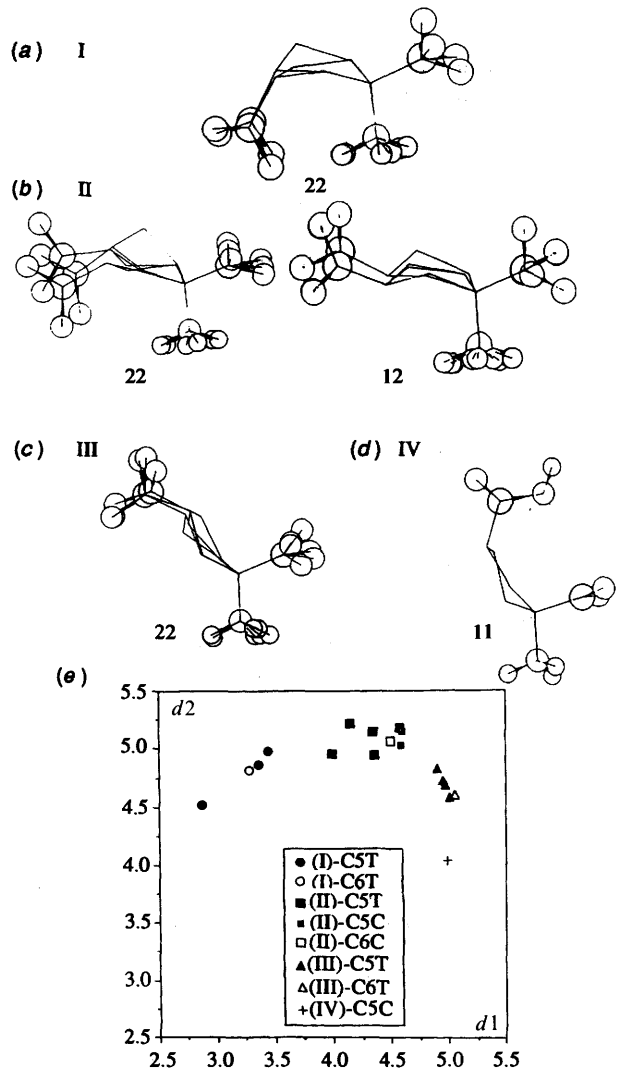

Fig. 12 Identification of four conformational families **I**–**IV** from the NMR and MD data of the two isomers analogues *cis*-**1** and *trans*-ACPD **2**; they are characterized by the distances, $d_1 = d_{N(\alpha)-C(\gamma)}$ and $d_2 = d_{C(\alpha)-C(\gamma)}$. The first two families display the α-NH_3^+ and γ-CO_2^- groups in a 'folded' form and the α-CO_2^- and γ-CO_2^- groups in an 'extended' one: (*a*) **I**, d_1 = 3.27–3.47 Å, d_2 = 4.92–4.98 Å, for **2** ($\mathbf{E}_1$, $\mathbf{E}_3$); (*b*) **II**, d_1 = 4.14–4.57 Å, d_2 = 5.18–5.22 Å, for **1** ($^2\mathbf{E}$, $^2\mathbf{T}_3$, $\mathbf{E}_3$) and **2** ($\mathbf{E}_4$, $^5\mathbf{E}$, $^4\mathbf{E}$). The two other families display the α-NH_3^+ and γ-CO_2^- groups in an 'extended' form and the α-CO_2^- and γ-CO_2^- groups in a 'folded' one: (*c*) **III**, d_1 = 4.9–4.99 Å, d_2 = 4.69–4.82 Å, for **2** ($\mathbf{E}_2$, $^3\mathbf{E}$, $^1\mathbf{E}$); (*d*) **IV**, d_1 = 4.99 Å, d_2 = 4.03 Å, for **1** ($\mathbf{E}_5$); (*e*) the different families for *cis*-C5 **1**, *trans*-C5 **2** and *cis*- and *trans*-C6 analogues are represented in a diagram according to their characteristic distances d_1 and d_2.

central nervous system, glutamine synthetase, D-glutamate-adding enzyme).

The superimposition shown in Fig. 11, of C(1) and of the central atoms of the two functional groups, *i.e.*, the α-N(1) and α-C(6) (α-CO_2^-), present for *cis*-C5 **1 2** a single type **II** of the potential active residues arrangement [Fig. 11(*b*)]. The interatomic distances between the pair of the free carboxyl αC(6)–γC(7) (5.17 Å) are longer than the pairs with the amino group αN–αC(6) (2.45 Å), αN–γC(7) (4.48 Å). Despite the presence of the ring in the compounds *cis*-C5 **1**, the γ-carboxyl groups of the 'extended' structures $^2\mathbf{E}$, $^2\mathbf{T}_3$ and $\mathbf{E}_3$, nearly overlap [Fig. 11(*b*)]. At alkaline pH [Fig. 11(*c*)], $^2\mathbf{E}$ is the single conformer identified, it also corresponds to the same type **II**. The main features of the type **II** can be considered as important elements for NMDA receptor recognition.

It is interesting to note that the most active compounds *trans*-C5 **2** in the series of potent ACPD-ligands have a negatively charged γ-carboxylate and an α-ammonium residue, close together on a short backbone. The region of *trans*-C5 **2** in which the 'folded' structure is maintained by electrostatic interaction constituted a particular conformational family (type **I**). The most important results obtained with *trans*-C5 **2** glutamic acid analogues are that the NH_3^+ protons are involved in an electrostatic interaction with the γ-carboxylate group (type **I**) in the $^1\mathbf{E}$, $\mathbf{E}_3$ and $^1\mathbf{T}_2$ structures [shown in Fig. 12(*a*)] sampled during MD simulations and in good agreement with NMR data. The most evident differences between this preponderant experimental NMR type-structure in solution and the averaged structure determined by combining all theoretical results (even the 'higher energies' ones) are displayed in Fig. 11(*e*). The superimposition shows that the oxygen atoms of the functional groups (γ-CO_2^-), sweep on three types of the potential active residues arrangement (types **I**, **II** and **III**). These *trans*-C5 analogues adopt multiple conformations and they allow the conformational classes **I**, **II** and **III** to be in qualitative agreement with the active form. The structures shown in Fig. 11(*e*) differ mainly in the arrangement of the glutamic acid analogue moieties, α-NH_3^+, α-CO_2^- and γ-CO_2^-, and illustrate the fact that the conformation at the receptor binding site might be relevant to 'higher energy' structures. Indeed the rigid *trans*-C6 isomer belongs to identical families **I** and **III** [Fig. 12(*e*)].

At physiological pH, the carboxylate groups bear no protons in the ionized state, however it will be noted that on the receptor, a negatively charged moiety with proton donor abilities could be necessary, thus each of the interacting atoms may establish multiple interactions with the atoms of the receptor. A conformational study was performed at isoelectric pH, on the zwitterionic molecule, in order to propose a different ligand conformational state which could play a key role in the efficiency of the interaction including hydrogen bonds. Consistent with literature data which argue against a charge delocalization between both oxygens of the γ-acid and in favour of a specific hydrogen bond between the distal acidic hydroxy and the receptor, compounds **1 1** and **2 1** were built and analysed by MD. The ionised functional groups now become γ-CO_2H, α-CO_2^-, α-NH_3^+ and may supply the system **1 2** or **2 2** with energy (to pass conformational barriers), to generate other conformers. In a model bound to the receptor by a proton donor or a water molecule, the resulting conformations may be characterized by different internuclear distances between Nα, Cα, Cγ shown in Fig. 11. At isoelectric pH [Fig. 11(*a*) and (*d*)], an electrostatic attraction between the 3-carboxy and the 1-carboxylate axial groups, led to 'folded' structures characterized by a short distance d_2 between the two carboxyl groups and belonging to the type **IV** for **1 1** [Fig. 11(*a*)] and to the type **III** for **2 1** [Fig. 11(*d*)]. The planes of the two acidic groups are 70–90° staggered relative to each other. This is the result of the ketonic oxygen [O(3)] and the negatively charged oxygen [O(4)] of the distal γ-acidic group, occupying different areas of space.

The (1*R*,3*S*)-*cis*-ACPD **1** would be recognized first by the NMDA receptor, at neutral pH, in the 'extended' major structure (type **II**) and supposing that protonation of the distal carboxylate occurs in the binding site, the ligand would enable folding into a type **IV** conformation in agreement with the pharmacophore suggested.[16a] The (1*S*,3*R*)-*trans*-ACPD **2** would be recognized first by the metabotropic receptor, at neutral pH, in the 'folded' major form (type **I**) and supposing that protonation of the distal carboxylate occurs in the binding site, the ligand would enable extension into a type **III** conformation in agreement with the pharmacophore defined.[16c]

These compounds can therefore be considered as interesting tools for further investigations on more bulky molecules with

the same potent activity. It was of interest that a detailed analysis allowed such a classification of the multiple possible conformations as they might be relevant to the receptor binding conformations.

Conclusions

The solution structure of cyclopentane-derived analogues of glutamic acid was determined by the combined use of NMR experimental results, mechanics and dynamics calculations, and theoretical simulation of NMR spectra. This study shows four conformational families **I–IV** with characteristic distances between the potentially active functional groups, d_1 (α-NH_3^+–γ-CO_2^-) and d_2 (α-CO_2^-–γ-CO_2^-). A different spatial conformation of the cyclopentane ring was found for the two isomers. The solution structure of *trans*-C5 **2** showed a different molecular arrangement from the X-ray conformation. In particular, we identified an electrostatic interaction which stabilizes a folded glutamic acid analogue moiety between the α-NH_3^+ and the γ-CO_2^- groups, at neutral pH (type **I**).

The results of ^1H and ^{13}C NMR spectroscopy and MD are in good agreement. The amino group in the *cis*-C5 **1** is found to be axial at all pH values (types **II** and **IV**); both carboxyl groups are preferentially equatorial ('extended') to reduce the steric energy (type **II**). In the *trans*-C5 **2** the steric parameters favour the conformer in which the dicarboxylate groups are equatorial or isoclinal at alkaline and acidic pH values (types **II** and **III**), while around pH 7, a 1,3-electrostatic attraction stabilizes the conformers with α-NH_3^+ and γ-CO_2^- in the axial or isoclinal position (essentially, type **I**).

A MD protocol that has been conceived with NMR data (on a different glutamate analogue), can be used directly and rapidly for the conformational analysis in water of other charged molecules of a similarly limited size however a protocol introducing explicit water molecules is the preferred choice, although the CPU times are longer. All the NMR and MD results allowed us to confirm the importance in the force field of the coulombic expression for these conformers. The electrostatic parameters are dependent upon the surrounding molecule, thus the conformational analysis deals properly with a specific solvent.

Both isomers are thus shown to adopt well defined conformations and prove to be well-adapted for comparative structure–activity correlation studies, the structural analysis being made in a solvent close to biological conditions. These five-membered molecules instead of cyclohexane derivatives in the previous study,[12] are more flexible and thus can adopt various conformations. These glutamate analogues have played an important role in defining the pharmacology of the various proteins involved in EAA-mediated synaptic transmission (EAA, excitatory amino acids). A better exploration of the binding site geometry is possible using conformational analysis of the pharmacophore. The data obtained may be considered as an important indication of the recognition features of these glutamic acid analogues in the biological systems considered (NMDA or ACPD receptors of the central nervous system, glutamine synthetase, D-glutamate-adding enzyme).

Experimental

Materials

cis-C5 **1** and *trans*-C5 **2** have been prepared previously in the laboratory.[13,17,29] Only racemates have been used for this work.

X-Ray crystallography

Crystal data for *trans*-C5 2 monohydrate. $C_7H_{11}NO_4 \cdot H_2O$, M 191.18. Monoclinic, a = 14.133(2), b = 10.691(2), c = 5.942(1) Å, β = 101.6(2)°, V = 879.5(7) Å^3, space group $P2_1/a$, Z = 4, D_c = 1.444 g cm^{-3}, final R-value 0.067, final R_w-value 0.071.

X-Ray structure determination of *trans*-C5 2 monohydrate. Crystals of compound **2** monohydrate were grown by slow evaporation of a potassium phosphate buffer–water solution at pH 4.5. Philips PW 1100 diffractometer, θ–2θ scan mode up to θ = 28°, graphite monochromated Mo-Kα radiation (λ = 0.710 69 Å); 2118 unique reflections; 652 reflections with $F \geq 7\sigma(F)$ considered observed. The structure was solved by SHELXS86 [30] and refined by full-matrix blocked least-squares with weight $w = 1/[\sigma^2(F) + 0.008\ F^2]$. The thermal parameters were anisotropic for all non-hydrogen atoms. The hydrogen atoms were all located on a difference-Fourier map and isotropically refined. All calculations were performed on a MicroVAX3400 Digital computer of the University of Padova using SHELX-76.[31]

Supplementary data. Tables of fractional atomic coordinates, bond lengths and bond angles are available from the Cambridge Crystallographic Data Centre.§

NMR spectroscopy

The samples were dissolved in deuterium oxide at a saturation concentration of approximately 0.01 mol dm^{-3}; the pH (in fact pD = pH −0.4, uncorrected here) was adjusted by addition of DCl or NaOD. At pH 7 the samples were dissolved in an aq. NaD_2PO_4–Na_2DPO_4 buffer (0.5 mol dm^{-3}), and it was possible to attain concentrations of 0.04 mol dm^{-3} for the ^1H experiments and 0.15 mol dm^{-3} for the ^{13}C experiments. Degassed and sealed tubes have been used for the T_1 determinations.

The errors on the chemical shifts are 0.01 and 0.1 ppm for ^1H and ^{13}C, respectively. A crystal of $TSPd_4$, 3-(trimethylsilyl)[2,2,3,3-$^2H_4$]propionic acid, sodium salt, [$^2H_4$]TSP was used as internal reference for the proton shifts, and for the carbon a value of the absolute frequency was used. The coupling constants are given with a precision of 0.5 Hz.

The experiments were run at 250 and 500 MHz for ^1H, and 62.9 MHz for ^{13}C, on Bruker WM 250 and AMX 500 Spectrometers, at room temperature. The data processing was done on a PC computer using the Bruker software WIN-NMR, and the spectrum simulation on a Macintosh II computer using the software NMR″II. Second-order spectra were calculated by an iterative method (Bruker PANIC program).

A presaturation of the solvent with two decoupling powers was used for all the 1D and 2D ^1H experiments.

The DEPT polarization transfer from ^1H to ^{13}C nuclei with decoupled spectra was acquired and tuned for optimum polarization transfer with the value of $^1J_{CH}$ = 135 Hz.

The 2D ^1H, ^1H COSY spectra were acquired with a spectral width of 1500 Hz into 512 data points in f_2, and with 64 experiments (f_1). The 90° pulse was 5.7 μs, the relaxation delay 1 s and each FID was acquired with 64 scans and 2 dummy-scans. The data were zero-filled to 1024 and 512 points in f_2 and f_1 respectively prior to double Fourier transformation with an unshifted sine-bell window function in both dimensions.

The 2D ^1H, ^{13}C COSY experiments data were acquired with a sweep width of 2500 Hz and 1024 data points, and 600 Hz and 64 data points (for ^1H and ^{13}C, respectively). The 90° pulses were 7.7 μs for ^1H and 12.0 μs for ^{13}C. Each FID was acquired with 512 scans and a relaxation delay of 1.2 s. This experiment gave ^1H decoupling in f_2 and C–H shift correlation with ^1H decoupling in the f_1 domain except for geminal ^2J. This experiment was tuned for optimum polarization transfer with again the value of $^1J_{CH}$ = 135 Hz.

§ For details of the CCDC deposition scheme, see 'Instructions for Authors (1995)', *J. Chem. Soc., Perkin Trans. 2*, 1995, issue 1.

The ^1H NOE difference spectra at 250 MHz were acquired automatically using one frequency list to define a series of irradiation points (on resonance) and one control (off-resonance). The individual FIDs were stored. Typically 4–5 irradiations were performed in one experiment with automatic cycling through the frequency list, using four dummy scans and 32 scans at each frequency. The pulse sequence used a relaxation delay (1.5 s) followed by a saturation time (2 s) using S3 = 40L power and then acquired data with the decoupler gated off. Difference spectra were obtained by the subtraction of the control (off-resonance saturation) from every other spectrum.

The ^{13}C T_1 relaxation times measurement used an inversion-recovery pulse sequence with a relaxation delay of 7 s and averaging 512 scans into a 16K data block. The experiment was repeated for 10 values of the variable delay (VD) ranging from 0.01 to 10 s. The T_1 values were calculated by using the Bruker DISNMR program. The calibrated value of the 180° pulse was 24.0 μs.

The 2D $J\delta$ selective INEPT using the polarization transfer from ^1H to ^{13}C gave long range heteronuclear coupling constants, $^3J(^{13}C–^1H)$. Measurement of long-range heteronuclear ($^{13}C–^1H$) coupling constants were performed on the AMX 500 spectrometer using 2D selective INEPT on a sample of 5 mg in 0.6 cm^3 of D_2O in 5 mm NMR tubes. The selective excitation of a proton signal allows detection of a single doublet for the corresponding coupled carbon(s). At 500 MHz, selectivity was achieved by a DANTE-type pulse train generated by the decoupler channel. The selectivity was equal to $\delta_{^1H} \pm 50$ Hz ($\gamma B/2\pi = 50$ Hz). The 90° non-selective proton pulses were 63 μs. A value of 50 ms for the Δ delay was optimum for J coupling of 3 Hz ($\Delta + P90° = 55$ ms). The relaxation delay was 1.3 s and each FID was acquired with 64 scans with broadband decoupling. 64 Experiments were achieved, and data were zero-filled to 256 points in the f_1 dimension. In the f_2 dimension, data were acquired with 2048 points, and no zero-filling was applied before Fourier transformation. The final resolutions were 0.12 and 15.25 Hz per point in the f_1 (J_{CH}) and f_2 (^{13}C chemical shifts) dimensions, respectively. Resolution enhancement by Gaussian transformation was carried out both in f_2 and f_1 dimensions. The $t_{1/2}$ was initially set to a value of 3 μs and was incremented by 17 ms per experiment.

Molecular dynamics

Molecular dynamics simulations were performed for *trans*-C5 and *cis*-C5 using the Biosym softwares INSIGHTII and DISCOVER [27] on a Silicon-Graphics Personal IRIS computer. The molecule was initially built from X-ray crystal data of *trans*-C5. Charges and atomic potentials were then redefined for the new molecule **2** using the built-in algorithm of the program.[32]

We used the CVFF Forcefield from Dauber–Osguthorpe [27] in which cross-terms represent the coupling of the deformations of internal coordinates and describe the coupling between adjacent bonds. These terms are required to reproduce accurately experimental vibrational frequencies and therefore the dynamic properties of molecules. A Morse function was used to describe the stretching of bonds.

For the electrostatic energies, when we constructed solvation boxes containing the C5 molecule and several water molecules using periodic boundary conditions, the relative permittivity was set to $\varepsilon = 1$, but if no explicit solvent molecules were incorporated during the run, the relative permittivity was set to be distance-dependent, $\varepsilon = R_{ij}$ ($\varepsilon = 5$), weighting more heavily short distance polarization interactions and damping long distance ones, to mimic the solvent effect.[33] For the same reason, no periodic-boundary conditions were required. A cut-off function was applied for non-bonded interactions, decreasing their effect smoothly between 18 and 20 Å, avoiding discontinuity and shortening the computation time. The neighbour list was recomputed every 10 iterations.

Newton's equations of motion were integrated every femtosecond and the rescaling of the temperature was controlled by the Verlet algorithm, too large a deviation from the target temperature is thus avoided.

The structures were first minimized using two different algorithms: steepest-descent for 200 iterations and then conjugate gradient until the first energy derivative was less than 0.1 kcal mol^{-1}. A preliminary run was performed with a 4 ps equilibration period, in which the system was coupled to a thermal bath [34] at 300 K to relieve strains in the structure and reach thermodynamic equilibrium. The simulation was then continued with a 8 ps period at 300 K followed by a temperature jump to 600 K for 4 ps. The dynamics were run for 42 ps (variable temperature) or 100 ps (constant temperature); the trajectory was sampled by minimizing and storing of the structure every picosecond.

The energies obtained with water boxes are those of C5 + $18H_2O$ systems; thus the energies of the minimized corresponding C5 molecules are evaluated ('steepest descent', one step) after the removal of the water molecules.

Coupling constants were calculated from the torsion angles using the software Altona on a Macintosh II computer.

Acknowledgements

We are grateful to B. Champion and Dr P. Ladam for helpful advice. This work was supported by grants from the DIAGNOSTICA STAGO-GEHT.

References

1 R. Chamberlain and R. Bridges, *Drug Design for Neuroscience*, ed. A. Kozikowski, Raven Press, New York, 1993, pp. 231–260.
2 D. T. Monoghan, R. J. Bridges and C. W. Cotman, *Ann. Rev. Pharmacol. Toxicol.*, 1989, **29**, 365; J. C. Watkins and H. J. Olverman, *Trends Neurosci.*, 1987, **10**, 265; R. H. Evans and J. C. Watkins, *Ann. Rev. Pharmacol. Toxicol.*, 1981, **21**, 165.
3 (*a*) F. Sladeczek, J. P. Pin, M. Recasens, J. Bockaert and S. Weiss, *Nature*, 1985, **317**, 717; F. Sladeczek, M. Recasens and J. Bockaert, *Trends Neurosci.*, 1988, **11**, 545; D. D. Schoepp, J. Bockaert and F. Sladeczek, *Trends Pharmacol. Sci.*, 1990, **11**, 508; (*b*) K. R. Stratton, P. F. Worley and J. Baraban, *Eur. J. Pharmacol.*, 1989, **173**, 235.
4 M. Masu, Y. Tanabe, K. Tsuchida, R. Shigamoto and S. Nakanishi, *Nature*, 1991, **349**, 760; Y. Tanabe, M. Masu, T. Ishii, R. Shigamoto and S. Nakanishi, *Neuron*, 1992, **8**, 169; K. M. Houamed, J. L. Kuijper, T. L. Gilbert, B. A. Haldeman, P. J. O'Hara, E. R. Mulvihill, W. Almers and F. S. Hagen, *Science*, 1991, **252**, 1318.
5 J. D. Gass and A. Meister, *Biochemistry*, 1970, **9**, 842.
6 F. Pratviel-Sosa, F. Acher, F. Trigalo, D. Blanot, R. Azerad and J. van Heijenoort, *FEMS Microbiology Letters*, 1994, **115**, 223.
7 H. J. Rogers, H. R. Perkins and J. B. Ward, *Microbiol Cell Walls and Membranes*, Chapman and Hall, London, 1980, pp. 239–297; J. van Heijenoort, *Bacterial Cell Walls*, ed. J. M. Ghuysen and R. Hackenbeck, Elsevier, 1994, pp. 39–54.
8 F. Pratviel-Sosa, D. Mangin-Lecreulx and J. van Heijenoort, *Eur. J. Biochem.*, 1991, **202**, 1169.
9 K. Shimamoto, M. Ishida, H. Shinozaki and Y. Ohfune, *J. Org. Chem.*, 1991, **56**, 4167.
10 (*a*) A. P. Kozikowski and A. H. Fauq, *Tetrahedron Lett.*, 1990, **31**, 2967; (*b*) M. Yanagida, K. Hashimoto, M. Ishida, H. Shionozaski and H. Shirahama, *Tetrahedron Lett.*, 1989, **30**, 3798; (*c*) C. Tsai, J. A. Schneider and J. Lehmann, *Neurosci. Lett.*, 1988, **29**, 6109; (*d*) K. Curry, M. J. Peet, D. S. K. Magnuson and H. McLennan, *J. Med. Chem.*, 1988, **31**, 864; (*e*) P. Hughes and J. Clardy, *J. Org. Chem.*, 1988, **53**, 4793; (*f*) J. Davies, R. H. Evans, A. A. Francis, A. W. Jones, D. A. S. Smith and J. C. Watkins, *Neurochem. Res.*, 1982, **7**, 1119.
11 (*a*) V. A. James, R. J. Walker and H. V. Wheal, *Br. J. Pharmacol.*, 1980, **68**, 711; (*b*) J. G. Hall, T. P. Hicks, H. McLennan, T. L. Richardson and H. V. Wheal, *J. Physiol.*, 1979, **286**, 29; (*c*)

H. V. Wheal and G. A. Kerkut, *Comp. Biochem. Physiol.*, 1976, **53C**, 51; (*d*) G. A. R. Johnston, D. R. Curtis, J. Davies and R. M. McCulloch, *Nature*, 1974, **248**, 804.
12 N. Morelle, J. Gharbi-Benarous, F. Acher, G. Valle, M. Crisma, C. Toniolo, R. Azerad and J. P. Girault, *J. Chem. Soc., Perkin Trans. 2*, 1993, 525; F. Acher, N. Morelle, J. Gharbi-Benarous, G. Valle, M. Crisma, C. Toniolo, R. Azerad and J. P. Girault, *Peptides*, 1993, 581.
13 (*a*) K. Curry, M. J. Peet, D. S. K. Magnuson and H. McLennan, *J. Med. Chem.*, 1988, **31**, 864; (*b*) K. Curry, *Can. J. Physiol. Pharmacol.*, 1991, **69**, 1076.
14 (*a*) E. Palmer, D. T. Monoghan and C. W. Cotman, *Eur. J. Pharmacol.*, 1989, **166**, 585; (*b*) M. A. Desai and J. P. Conn, *Neurosci. Lett.*, 1990, **109**, 157; (*c*) A. J. Irving, J. G. Schofield, D. C. Sunter and G. L. Collingridge, *Eur. J. Pharmacol.*, 1990, **186**, 363.
15 O. Manzoni, L. Prezeau, F. A. Rassendren, F. Sladeczek, K. Curry and J. Bockaert, *Mol. Pharmacol.*, 1992, **42**, 322.
16 (*a*) D. F. Ortwine, T. C. Malone, C. F. Bigge, J. T. Drummond, C. Humblet, G. Johnson and G. W. Pinter, *J. Med. Chem.*, 1992, **35**, 1345; (*b*) P. J. O'Hara, P. O. Sheppard, M. Thogersen, D. Venezia, B. A. Haldeman, V. McCrane, K. M. Houamed, C. Thomsen, T. L. Gilbert and E. R. Mulvihill, *Neuron.*, 1993, **11**, 41; (*c*) G. Costantino, B. Natalini, R. Pellicciari, F. Moroni and G. Lombardi, *Bioorg. Med. Chem.*, 1993, **4**, 259.
17 F. Trigalo, D. Buisson and R. Azerad, *Tetrahedron Lett.*, 1988, **29**, 6109.
18 (*a*) R. Bucourt, *Top. Stereochem.*, 1974, **8**, 159; (*b*) B. Testa, *Principles of Organic Stereochemistry*, Dekker, New York, 1979, pp. 112–113; D. Cremer, *Isr. J. Chem.*, 1980, **20**, 12; (*c*) B. Fuchs, *Top. Stereochem.*, 1978, **10**, 1.
19 (*a*) D. Cremer and J. A. Pople, *J. Am. Chem. Soc.*, 1975, **97**, 1354; (*b*) J. B. Lambert, J. J. Papaye, S. A. Khan, K. A. Kappauf and E. S. Magyar, *J. Am. Chem. Soc.*, 1974, **96**, 6112; (*c*) C. Altona and M. Sundaralingam, *J. Am. Chem. Soc.*, 1972, **94**, 8205; C. Altona, *Recl. Trav. Chim. Pays-Bas*, 1982, **101**, 413.
20 M. R. Bendall and D. T. Pegg, *J. Magn. Reson.*, 1983, **53**, 272.
21 (*a*) A. Bax and R. Freeman, *J. Magn. Reson.*, 1981, **44**, 542; (*b*) P. Barker and R. Freeman, *J. Magn. Reson.*, 1985, **64**, 334.
22 J. A. Rutar, *J. Magn. Reson.*, 1984, **59**, 306; T. C. Wong and V. Rutar, *J. Am. Chem. Soc.*, 1984, **106**, 7380.
23 (*a*) P. Ladam, J. Gharbi-Benarous, M. Pioto, M. Delaforge and J. P. Girault, *Magn. Reson. Chem.*, 1994, **32**, 1; (*b*) T. Jippo, O. Kamo and K. Nagayama, *J. Magn. Reson.*, 1986, **66**, 344.
24 (*a*) C. Altona and M. Sundaralingam, *J. Am. Chem. Soc.*, 1973, **95**, 2333; (*b*) C. A. G. Haasnoot, F. A. A. M. de Leeuw and C. Altona, *Tetrahedron*, 1980, **36**, 2783.
25 I. Tvaroska, M. Hricovini and E. Petrakova, *Carbohydr. Res.*, 1989, **189**, 359.
26 A. Allerhand, D. Doddrell and R. Komoroski, *J. Chem. Phys.*, 1971, **55**, 189; J. R. Lyerla and G. C. Levy, *Top. Carbon-13 NMR Spectrosc.*, 1974, **1**, 79.
27 P. Dauber-Osguthorpe, V. A. Roberts, D. J. Osguthorpe, J. Wolff, M. Genest and A. T. Hagler, *Proteins: Struct., Funct. and Genet.*, 1988, **4**, 31.
28 S. K. Burt, D. Mackay and A. T. Nagler, in *Comput.-Aided Drug Design*, ed. T. J. Perun and C. L. Propst, Marcel Dekker, New York and Basel, 1989, p. 66.
29 R. A. Stephani, W. B. Rowe, J. D. Gass and A. Meister, *Biochemistry*, 1972, **11**, 4094.
30 G. M. Sheldrick, SHELXS 86, Program for Crystal Structure Determination, University of Göttingen, 1986.
31 G. M. Sheldrick, SHELX-76, Program for Crystal Structure Determination, University of Cambridge, 1976.
32 U. Dinur and A. T. Hagler, *J. Chem. Phys.*, 1989, **91**, 2949.
33 P. Kollmann, *J. Am. Chem. Soc.*, 1984, **106**, 765.
34 H. J. C. Berendsen, J. P. M. Postma, W. F. van Gunsteren, A. DiNola and J. R. Haak, *J. Chem. Phys.*, 1984, **81**, 3684.

Paper 4/07250B
Received 28*th November* 1994
Accepted 16*th January* 1995